Nonlinear output-feedback control of torsional vibrations in drilling systems

INTERNATIONAL JOURNAL OF ROBUST AND NONLINEAR CONTROL
Int. J. Robust Nonlinear Control 2017; **27**:3659–3684
Published online 26 January 2017 in Wiley Online Library (wileyonlinelibrary.com). DOI: 10.1002/rnc.3759

Nonlinear output-feedback control of torsional vibrations in drilling systems

T. Vromen[1,*,†], N. van de Wouw[1,2,3], A. Doris[4], P. Astrid[5] and H. Nijmeijer[1]

[1]*Department of Mechanical Engineering, Eindhoven University of Technology, 5600 MB, Eindhoven, The Netherlands*
[2]*Department of Civil, Environmental & Geo-Engineering, University of Minnesota, Minneapolis, USA*
[3]*Delft Center for Systems and Control, Delft University of Technology, Delft, The Netherlands*
[4]*Well Engineering Design, Nederlandse Aardolie Maatschappij B.V. (NAM), The Netherlands*
[5]*Wells R&D, Shell Global Solutions International B.V., Rijswijk, The Netherlands*

SUMMARY

This paper considers the design of a nonlinear observer-based output-feedback controller for oil-field drill-string systems aiming to eliminate (torsional) stick–slip oscillations. Such vibrations decrease the performance and reliability of drilling systems and can ultimately lead to system failure. Current industrial controllers regularly fail to eliminate stick–slip vibrations under increasingly challenging operating conditions caused by the tendency towards drilling deeper and inclined wells, where multiple vibrational modes play a role in the occurrence of stick–slip vibrations. As a basis for controller synthesis, a multi-modal model of the torsional drill-string dynamics for a real rig is employed, and a bit–rock interaction model with severe velocity-weakening effect is used. The proposed model-based controller design methodology consists of a state-feedback controller and a (nonlinear) observer. Conditions, guaranteeing asymptotic stability of the desired equilibrium, corresponding to nominal drilling operation, are presented. The proposed control strategy has a significant advantage over existing vibration control systems as it can effectively cope with multiple modes of torsional vibration. Case study results using the proposed control strategy show that stick–slip oscillations can indeed be eliminated in realistic drilling scenarios in which industrial controllers fail to do so. Moreover, key robustness aspects of the control system involving the robustness against uncertainties in the bit–rock interaction and changing operational conditions are evidenced.

Received 16 December 2015; Revised 16 July 2016; Accepted 5 January 2017

KEY WORDS: stick–slip oscillations; output-feedback; observer-based; drilling systems

1. INTRODUCTION

Drilling systems are used to drill deep wells for the exploration and production of oil and gas, mineral resources and geo-thermal energy. Such a drilling system is schematically shown in Figure 1. Surface and down-hole measurements [1–4] indicate that these systems experience different types of oscillations, which significantly decrease the drilling rate-of-penetration and can damage the drill bit (e.g. bit tooth wear), the drill pipes (e.g. twisted drill pipe) and the bottom hole assembly. Different modes of vibration, such as axial, lateral and torsional vibrations, lead to bit bouncing, whirling and torsional stick–slip, respectively. The focus of the current paper is on the aspect of mitigation of torsional stick–slip oscillations by means of control as these vibrations are known to be highly detrimental to drilling efficiency, reliability, and safety.

*Correspondence to: T. Vromen, Eindhoven University of Technology, Department of Mechanical Engineering, 5600 MB Eindhoven, The Netherlands.
†E-mail: t.g.m.vromen@tue.nl

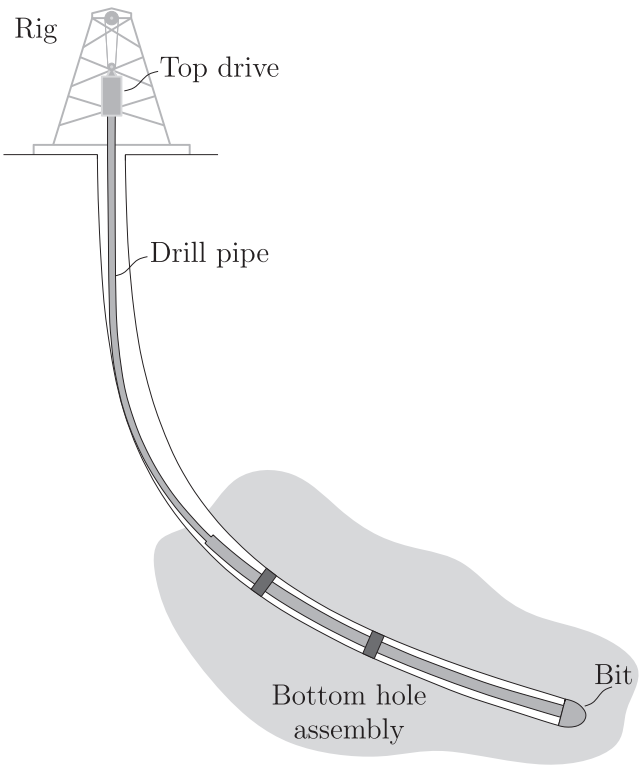

Figure 1. Schematic drilling system (adapted from [26]).

So as to support the design of controllers to eliminate torsional vibrations, most studies rely on one or two degree-of-freedom (DOF) models for the torsional drill-string dynamics only, e.g., [5–10]. In these models, it is generally assumed that the resisting torque at the bit–rock interface can be modelled as a frictional contact with a velocity-weakening effect as reported in [11, 12]. However, experiments using single cutters, aiming at the identification of the bit–rock interaction law, have not revealed any velocity-weakening effect [13]. In fact, modelling of the coupled axial and torsional dynamics, as for example in [14–17], shows that the velocity-weakening effect in the torque-on-bit (TOB) is a consequence of the drilling dynamics, rather than an intrinsic property of the bit–rock interface. The fact that such coupling effectively leads to a velocity-weakening effect of the TOB (e.g., [15, 16]) motivates to adopt a modelling-for-control approach for drill-string dynamics involving the torsional dynamics only, while including velocity-weakening in the bit–rock interaction law, as we will pursue in this paper. To model the torsional drill-string dynamics, we use a finite-element method (FEM) representation of the drill-string. A different modelling approach that is taken in [18, 19], where infinite-dimensional models, formulated in terms of partial differential equations, are considered. Using the same approach as a basis, models in terms of delay-differential equations are derived in [20–23]. In [24], it is shown that discretizations of such infinite-dimensional models resulting in a finite-element representation of the drill-string dynamics can accurately describe the underlying drill-string dynamics leading to torsional vibrations. Therefore, we will use such an FEM model of the drill-string dynamics as a basis for the model-based controller design methodology proposed in this paper. The proposed FEM drill-string model (Section 2) of the torsional dynamics, with a velocity-weakening bit–rock interaction law, has been validated with field data under different conditions (such as weight-on-bit (WOB) and angular velocity)[25].

Different control strategies aiming to suppress torsional vibrations can be found in the literature. In [9], the use of torque feedback in addition to a speed controller is investigated. The underlying idea is making the top rotary system behave in a 'soft' manner, hence the name *Soft Torque Rotary System*, see also [5]. In these works, it is assumed that the drilling system behaves like a 2-DOF torsional pendulum of which the first torsional mode can be damped using a PI-controller based

DOI: 10.1002/rnc

on feedback of the surface angular velocity. In [12, 27], the aforementioned SoftTorque approach is compared with a control method on the basis of torsional rectification, which outperforms the SoftTorque approach in simulation studies by using improved torque feedback on the basis of the twist of the drill-string near the rotary table. Another type of PI-controller is developed in [28], using a 3-DOF drill-string model for controller design. To do so, it is assumed that the bit angular velocity can be measured. We care to stress that down-hole measurements for real-time control purposes are not available in practice. A linear $\mathcal{H}_\infty$ controller synthesis approach is presented in [6]. Herein, the bit–rock interaction, key in causing stick–slip, is not taken into account in the controller design and stability analysis of the closed-loop dynamics. A control design approach, where information of the nonlinear bit–rock interaction model is explicitly taken into account in the controller synthesis, is proposed in [7, 29, 30]. Drawbacks of the approaches in [6, 7] are, firstly, the necessity of down-hole measurements reflecting the twist of the drill-string between surface and bit, which can not be measured in practice, and, secondly, the fact that only one torsional mode of the drill-string is taken into account.

Increasing demands on the operating envelope and a tendency towards drilling deeper and inclined wells impose higher demands on the controllers used in drilling systems. As a consequence, industrial controllers (such as SoftTorque) are not always able to eliminate stick–slip vibrations under the imposed operating conditions [31, 32]. Two main reasons for this deficiency are the influence of multiple dynamical modes of the drill-string on torsional vibrations [32, 33] and the uncertainty in the bit–rock interaction law.

The main contribution of this paper is a nonlinear output-feedback control strategy mitigating torsional stick–slip vibrations while (i) only using surface measurements, that is, the top drive angular velocity, (ii) taking into account a multi-modal drill-string model and (iii) accounting for severe velocity-weakening and uncertainty in the bit–rock interaction. A preliminary version of this work has been presented in [34]. Additional contributions of the current paper are, firstly, an extensive robustness analysis of the proposed controller, secondly, validation of the proposed control strategy by application to a high-order FEM model of the drill-string dynamics and, thirdly, a complete proof regarding the stability properties of the closed-loop system. The robustness analysis mainly focuses on implementation aspects essential in practice, such as changing dynamics owing to the increasing length of the drill-string and changing conditions at the bit–rock interface (e.g., due to changing formation characteristics or bit wear).

This paper is organized as follows. Section 2 introduces the drill-string model on the basis of a finite-element model of a real-life rig, and a reduced-order model is derived to facilitate controller design. Subsequently, in Section 3, the control problem is formulated. Next, in Section 4, we present a design approach for nonlinear output-feedback controllers including a robust stability analysis of the resulting (reduced-order) closed-loop system. Section 5 presents simulation results illustrating the effectiveness of the proposed approach applied to the reduced-order drill-string model. In Section 6, the controller design strategy is validated by application to the full-scale finite-element drill-string model and a stability analysis of the closed-loop system is performed. Next, in Section 7, the robustness of the controller is investigated by means of simulation case studies involving realistic drilling scenarios. Finally, the main results of this work are discussed in Section 8.

1.1. Preliminaries

In support of the controller design result in Section 4.1, we present the following definitions on input-to-state-stability (ISS) and the strict passivity property. The concept of input-to-state stability has been introduced in [35]. Its local version has first appeared in [36].

Definition 1

The system $\dot{x}(t) \in F(x(t), e(t))$ is locally input-to-state stable (LISS) with respect to the input $e(t)$ if there exist constants $c_1, c_2 > 0$, a function ρ of class $\mathcal{KL}$ and a function μ of class $\mathcal{K}^{\ddagger}$ such

[‡]A function $\alpha : \mathbb{R}_{\geqslant 0} \to \mathbb{R}_{\geqslant 0}$ belongs to class $\mathcal{K}$ if it is continuous, zero at zero, and strictly increasing. It is said to belong to class $\mathcal{K}_\infty$ if it is unbounded, that is, $\alpha(r) \to \infty$ as $r \to \infty$. A function $\beta : \mathbb{R}_{\geqslant 0} \times \mathbb{R}_{\geqslant 0} \to \mathbb{R}_{\geqslant 0}$ belongs to class $\mathcal{KL}$ if $\beta(\cdot, s)$ is of class $\mathcal{K}$ for each $s \geqslant 0$, $\beta(r, \cdot)$ is decreasing and $\beta(r, s) \to 0$ as $s \to \infty$.

DOI: 10.1002/rnc

that for each initial condition $x(0) = x_0$, such that $\|x_0\| \leqslant c_1$, and each piecewise continuous bounded input function $e(t)$ defined on $[0, \infty)$ and satisfying $\sup_{\tau\in[0,\infty)} \|e(\tau)\| \leqslant c_2$, it holds that; all solutions $x(t)$ exist on $[0, \infty)$ and, all solutions satisfy

$$\|x(t)\| \leqslant \rho\left(\|x_0\|, t\right) + \mu\left(\sup_{\tau\in[0,t]} \|e(\tau)\|\right), \ \forall t \geqslant 0. \tag{1}$$

Consider the linear time-invariant minimal state-space system

$$\begin{aligned} \dot{x} &= Ax + Gv \\ q &= Hx + Dv \end{aligned} \tag{2}$$

with the state $x \in \mathbb{R}^n$, and input and output $v, q \in \mathbb{R}$.

Definition 2 ([37]*)*
System (2) or the quadruple (A, G, H, D) is said to be strictly passive if there exist an $\varepsilon > 0$ and a matrix $P = P^\top > 0$ such that

$$\begin{bmatrix} A^\top P + PA + \varepsilon I & PG - H^\top \\ G^\top P - H & -D - D^\top \end{bmatrix} \leqslant 0. \tag{3}$$

2. DRILL-STRING DYNAMICS MODEL

The system under study is a realistic drill-string model of a jack-up drilling rig. With this drilling rig, the reservoir sections of the wells are drilled with a 6" bit to reach depths of more then 6000 m and with an inclination angle up to 60°, resulting in significant resistive torques along the drill-string. The rig is equipped with a modern SoftTorque system [38]. However, for this depth and hole size stick–slip vibrations have been observed in the field for this rig [39]. A finite-element model of this drilling system has been developed, and the simulation results of this model have been validated with field data under different conditions (such as WOB and angular velocity), see [25]. This finite-element drill-string model is the basis for controller design in Section 6 and a robustness analysis based on simulation studies as presented in Section 7.

The finite-element method is used to construct a multi-modal torsional drill-string model (with 18 elements). The top-side element is a rotational inertia to model the top drive inertia, the subsequent elements represent equivalent pipe sections on the basis of the dimensions and material properties of the drill-string; see [25] for more details. The resulting model can be written as

$$M\ddot{\theta} + D\dot{\theta} + K_t\theta_d = S_w T_w(\dot{\theta}) + S_b T_{bit}(\dot{\theta}_1) + S_t T_{td} \tag{4}$$

with the angular coordinates $\theta \in \mathbb{R}^m$, where $m = 18$, the top drive motor torque input $T_{td} \in \mathbb{R}$ being the control input, the bit–rock interaction torque $T_{bit} \in \mathbb{R}$ and the interaction torques $T_w \in \mathbb{R}^{m-1}$ between the borehole and the drill-string acting on the nodes of the FEM model. The interaction torques T_w express the effect of the drag along the drill-string and the well geometry (especially at build and drop sections) depending on the angular velocity of the drill-string. The coordinates θ represent the angular displacements of the nodes of the finite-element representation. Next, we define the difference in angular position between adjacent nodes as follows: $\theta_d := \begin{bmatrix} \theta_1 - \theta_2 & \theta_2 - \theta_3 & \cdots & \theta_{17} - \theta_{18} \end{bmatrix}^\top$. In (4), the mass, damping and 'stiffness' matrices are, respectively, given by $M \in \mathbb{R}^{m\times m}$, $D \in \mathbb{R}^{m\times m}$ and $K_t \in \mathbb{R}^{m\times m-1}$. The matrices $S_w \in \mathbb{R}^{m\times m-1}$, $S_b \in \mathbb{R}^{m\times 1}$ and $S_t \in \mathbb{R}^{m\times 1}$ represent the generalized force directions of the interaction torques, the bit torque and the input torque, respectively. The coordinates θ are chosen such that the first element (θ_1) describes the rotation of the bit and the last element (θ_{18}) the rotation of the top drive at surface. The interaction between the borehole and the drill-string is modelled as Coulomb friction, that is,

$$T_{w,i} \in T_i \ \text{Sign}\left(\dot{\theta}_i\right), \quad \text{for } i = 2, \ldots, 18, \tag{5}$$

DOI: 10.1002/rnc

with T_i representing the amount of friction at each element and the set-valued sign function Sign $(\cdot)$ defined as

$$\text{Sign}\,(y) \triangleq \begin{cases} -1, & y < 0 \\ [-1, 1]\,, & y = 0 \\ 1, & y > 0. \end{cases} \tag{6}$$

The bit–rock interaction model, including the velocity-weakening effect, is given by

$$T_{bit}(\dot{\theta}_1) \in \text{Sign}\left(\dot{\theta}_1\right)\left(T_d + (T_s - T_d)\, e^{-v_d|\dot{\theta}_1|}\right) \tag{7}$$

with T_s the static torque, T_d the dynamic torque, and $v_d := \frac{30}{N_d \pi}$ indicating the decrease from static to dynamic torque. For this model, the parameters are also on the basis of the comparison between the simulation results and the (surface) field data as shown in [25]. The values of the parameters are given by $T_s = 7700$ Nm, $T_d = 1700$ Nm, $N_d = 5$ rpm, and the resulting bit–rock interaction model is shown in Figure 2. Note that, in practice, T_s and T_d can also be measured directly on the basis of well data obtained with the drill-string off/on bottom. In the off bottom situation, the drill-string is rotating and the drill bit is not penetrating the rock, while on bottom describes the situation when the drill bit is penetrating the rock. The model (4), (5) and (7) together forms a differential inclusion that can be written in state-space Lur'e-type form as follows:

$$\begin{aligned} \dot{x} &= Ax + Bu_t + Gv + G_2 v_2 \\ q &= Hx \\ q_2 &= H_2 x \\ y &= Cx \\ v &\in -\varphi(q) \\ v_2 &\in -\phi(q_2), \end{aligned} \tag{8}$$

where $x := \left[\, \theta_d \;\; \dot{\theta} \,\right]^\top \in \mathbb{R}^{35}$ is the state. Moreover, $q := \omega_{bit} \in \mathbb{R}$, with $\omega_{bit} := \dot{\theta}_1$ the angular velocity of the bit, and $q_2 := \left[\, \dot{\theta}_2 \;\cdots\; \dot{\theta}_{18} \,\right]^\top \in \mathbb{R}^{17}$ are the angular velocity arguments of the set-valued nonlinearities φ and ϕ, respectively. The bit–rock interaction torque is given by $v \in \mathbb{R}$, and the drill-string-borehole interaction torques are given by $v_2 \in \mathbb{R}^{17}$. Furthermore, $u_t := T_{td} \in \mathbb{R}$ is the control input and $y := \omega_{td} \in \mathbb{R}$, with $\omega_{td} := \dot{\theta}_{18}$ the angular velocity of the top drive, is the measured output, which implies that only surface measurements will be employed in the output-feedback control strategy to be proposed in Section 4. The matrices A, B, C, G, G_2, H and H_2 in (8), with appropriate dimensions, are given by

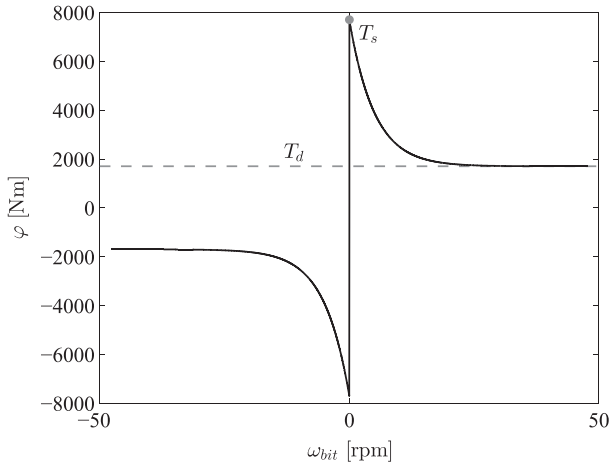

Figure 2. Bit–rock interaction model.

DOI: 10.1002/rnc

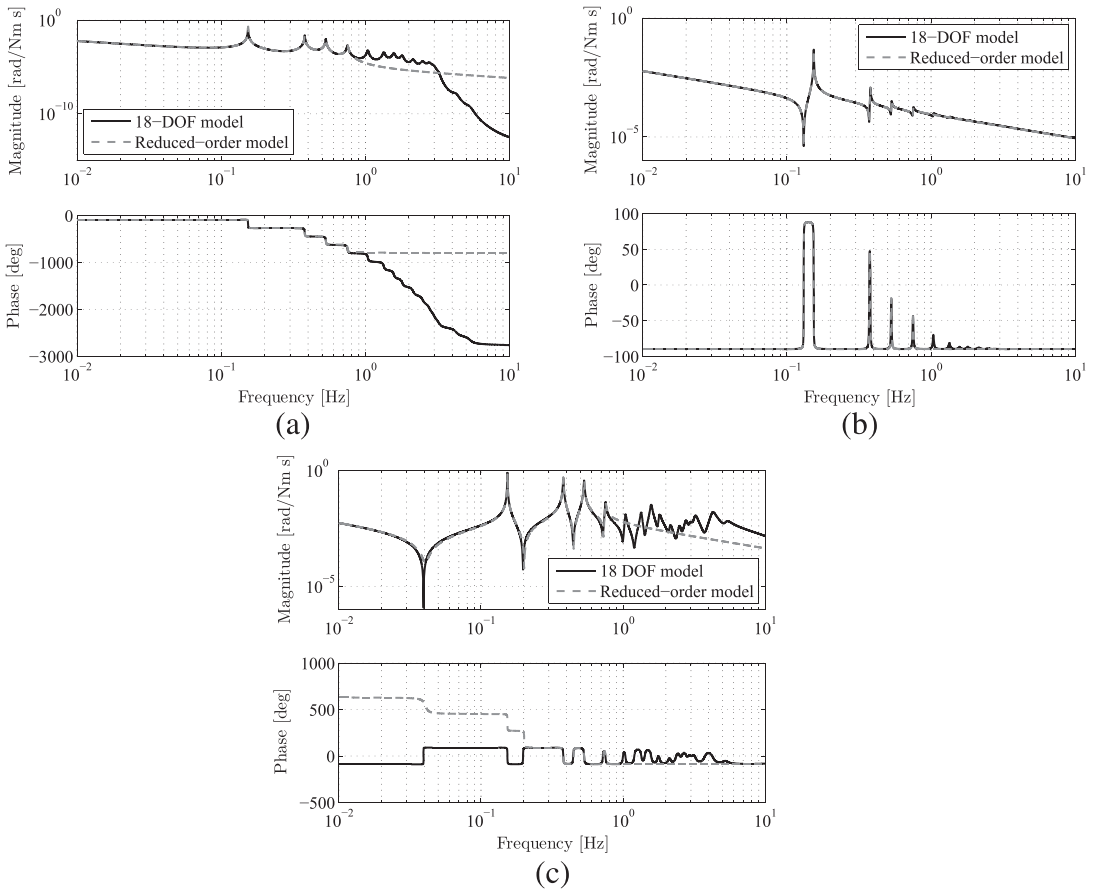

Figure 3. Frequency response functions of the full-order and reduced-order model, (a) from input torque T_{td} to bit velocity ω_{bit} (b) from input torque T_{td} to top drive velocity ω_{td} and (c) from bit torque T_{bit} to bit velocity ω_{bit}, that is, the bit-mobility.

$$A = \begin{bmatrix} O_{17\times 17} & a \\ -M^{-1}K_t & -M^{-1}D \end{bmatrix},\ a = \begin{bmatrix} 1 & -1 & 0 & \cdots & 0 \\ 0 & \ddots & \ddots & \ddots & \vdots \\ \vdots & \ddots & \ddots & \ddots & 0 \\ 0 & \cdots & 0 & 1 & -1 \end{bmatrix},\ B = \begin{bmatrix} O_{17\times 1} \\ M^{-1}S_t \end{bmatrix},\ C = \begin{bmatrix} O_{1\times 34} & 1 \end{bmatrix},$$

$$G = \begin{bmatrix} O_{17\times 1} \\ M^{-1}S_b \end{bmatrix},\ G_2 = \begin{bmatrix} O_{17\times 17} \\ M^{-1}S_w \end{bmatrix},\ H = \begin{bmatrix} O_{1\times 17} & 1 & O_{1\times 17} \end{bmatrix},\ H_2 = \begin{bmatrix} O_{17\times 18} & I_{17} \end{bmatrix}$$

with I_k the k-by-k identity matrix and $O_{k\times l}$ a k-by-l matrix with all zero entries. Note that $\varphi(q) := T_{bit}(\omega_{bit})$ and $\phi(q_2) := \begin{bmatrix} T_{w,2}(\dot{\theta}_2) & \cdots & T_{w,18}(\dot{\theta}_{18}) \end{bmatrix}^\top$. The relevant frequency response functions of (the linear part of) system (8) from inputs T_{td} and T_{bit} to the outputs ω_{td} and ω_{bit} are shown in Figure 3.

2.1. Reduced-order model

In order to both facilitate the design of and to decrease the implementation burden of the resulting observer-based output-feedback controllers (Section 4), we apply model reduction to obtain a low-order approximation of the drilling system dynamics (8). We will use the model reduction approach for Lur'e-type systems as proposed in [40], which employs a linear model reduction technique (such as balanced truncation) for the reduction of the linear part of the Lur'e-type system, while leaving the nonlinearity unchanged. The linear part of such a reduced-order model approximates the input–output behavior from inputs u_t and v to outputs y and q. The inputs and outputs related to the drill–string–borehole interaction ($T_{w,i}$) are not taken into account in the reduction process but can

DOI: 10.1002/rnc

be approximated using the transformation matrix obtained from the reduction procedure. So as to support such reduction approach, system (8) is represented as a Lur'e type system $\Sigma = \left(\Sigma^{lin}, \varphi\right)$, consisting of high-order linear dynamics Σ^{lin} with a single static output-dependent nonlinearity φ, related to the bit–rock interaction, in the feedback loop. We combine the inputs u_t and v and the outputs y and q, yielding the new input matrix $\begin{bmatrix} B & G \end{bmatrix}$ and the new output matrix $\begin{bmatrix} C^\top & H^\top \end{bmatrix}^\top$. With these inputs and outputs, applying balanced truncation to the linear part of the Lur'e-type system results in the reduced-order linear system Σ_r^{lin}. Now, the reduced-order linear part is interconnected with the original nonlinearity yielding the nonlinear reduced-order drill-string system model $\Sigma_r = \left(\Sigma_r^{lin}, \varphi\right)$. An important advantage of this method in the scope of control design is the fact that the relevant input–output behavior is approximated by the reduced-order model, resulting in a low-order approximation of the drill-string dynamics that is instrumental in the scope of controller synthesis.

Using the approach outlined above, we obtain a reduced-order model with state $x_r \in \mathbb{R}^{m_r}$, with $m_r = 9$. The equations of motion for the reduced-order system are written as (now again taking into account drill-string–borehole interactions):

$$\begin{aligned} \dot{x}_r &= A_r x_r + B_r u_t + G_r v_r + G_{2,r} v_{2,r} \\ q_r &= H_r x_r \\ q_{2,r} &= H_{2,r} x_r \\ y_r &= C_r x_r \\ v_r &\in -\varphi(q_r) \\ v_{2,r} &\in -\phi(q_{2,r}) \end{aligned} \tag{9}$$

and the bit–rock interaction as in (7) and as shown in Figure 2. The relevant frequency response functions for the linear part of the reduced-order dynamics in (9) are shown in Figure 3. Clearly, the first four resonance modes (and the rigid-body mode) are accurately captured in the reduced-order model. The so-called bit-mobility, shown in Figure 3(c), describes the dynamics of the drill-string system from bit torque input (T_{bit}) to bit angular velocity output (ω_{bit}). In other words, it indicates the sensitivity of the bit angular velocity for disturbances in the bit–rock interaction torque. A lower magnitude of the bit-mobility makes the drill-string system thus less sensitive for disturbances at the bit (induced by the bit–rock interaction including a destabilizing velocity-weakening effect) that could eventually lead to stick–slip oscillations. Therefore, the bit-mobility gives an indication of the most important resonance modes in the onset of stick–slip vibrations. It can be seen that the first three resonance modes are dominant in the bit-mobility. In this paper, we have chosen for a reduced-order model with $m_r = 9$, which actually captures the first four flexibility modes. This choice for $m_r = 9$ is such that, on the one hand, it is sufficiently large to capture the dominant modes and thereby limiting the model error owing to reduction as much as possible, while, on the other hand, the model order is limited to support controller and observer design. Note that the first three flexibility modes are often responsible for down-hole torsional vibrations of drill-strings with a length above 5 km that are used for 6" hole sections. These drill-strings are tapper strings with $3\frac{1}{2}$" and 5" drill pipes, and this drill-string configuration is quite common for many wells around the globe.

3. CONTROL PROBLEM FORMULATION

In Section 3.1, we formulate the control problem and specify the underlying controller objectives. Additionally, in Section 3.2, we apply a loop transformation to the model in (9) to render it amendable for controller design, to be discussed in detail in Section 4.

3.1. Controller objectives

The objective is to regulate the nonlinear drill-string system to a constant angular velocity setpoint (ω_{eq}) by means of an observer-based output-feedback controller. The available measurement for the

DOI: 10.1002/rnc

controller is the top drive angular velocity $y = \omega_{td}$, and the system can be controlled by the top drive torque $u_t = T_{td}$. As briefly mentioned in the introduction, the controller should

(1) (locally) stabilize the constant rotational velocity ω_{eq} of the drill-string, therewith eliminating torsional (stick–slip) vibrations;
(2) be able to deal with severe velocity-weakening and uncertainty in the nonlinear bit–rock interaction φ;
(3) be applicable to multi-modal drill-string models, that is, effectively deal with flexibility modes at higher frequencies.

3.2. Model reformulation

So as to facilitate controller synthesis, the drill-string dynamics (9) are rewritten in a specific form. The desired constant angular velocity $\omega_{eq} > 0$ can be associated with a desired equilibrium $x_{r,eq}$ for the state of the system. So as to ensure that $x_{r,eq}$ is indeed an equilibrium of the closed-loop system, the control input $u_t = u_c + \tilde{u}$ is decomposed in a constant feedforward torque u_c (inducing $x_{r,eq}$) and the feedback control input $\tilde{u}$. If we assume that we can indeed operate the drill-string system at positive angular velocity, the Coulomb friction terms $T_{w,i}$ along the drill-string do not affect the dynamics of the system, at least locally near the desired operating condition and can consequently be represented by constant resistive torques. These constant resistive torques can then be compensated by the feedforward torque u_c. The equilibrium $x_{r,eq}$ and feedforward torque u_c can be obtained from the equilibrium condition of system (9) that has to satisfy the algebraic inclusion

$$A_r x_{r,eq} - G_r \varphi \left(H_r x_{r,eq}\right) - G_{2,r} \phi \left(H_{2,r} x_{r,eq}\right) + B_r u_c \ni 0. \tag{10}$$

In addition, we require $y_{r,eq} = C_r x_{r,eq} = \omega_{eq}$. Consequently, $q_{r,eq} = H_r x_{r,eq}$ will probably not exactly match ω_{eq}, because owing to the reduction (Section 2.1), the equilibrium outputs $q_{r,eq}$ and $y_{r,eq}$ of the reduced-order model are not necessarily exactly equal. The latter is caused by the reduction error introduced by the model reduction procedure. In the simulation results, in Section 5, it is shown that this reduction error is small.

Next, we write the reduced-order drill-string system (9) in perturbation states ξ_r with respect to the equilibrium, defined as $\xi_r := x_r - x_{r,eq}$. Furthermore, we apply a linear loop transformation to change the properties of the nonlinearity φ in order to satisfy certain conditions related to the controller design in Section 4. The combined coordinate and loop transformation results in the state-space representation of the dynamics in perturbation coordinates given by

$$\begin{aligned} \dot{\xi}_r &= A_{r,t}\xi_r + B_r\tilde{u} + G_r\tilde{v}_r \\ \tilde{q}_r &= H_r\xi_r \\ \tilde{y}_r &= C_r\xi_r \\ \tilde{v}_r &\in -\tilde{\varphi}_r\left(\tilde{q}_r\right), \end{aligned} \tag{11}$$

where we define $A_{r,t} := A_r + \delta G_r H_r$ with $\delta > 0$ a constant to apply the linear loop transformation. Moreover, $\tilde{q}_r := q_r - H_r x_{r,eq}$, $\tilde{y}_r := y_r - C_r x_{r,eq}$, $\tilde{\varphi}_r\left(\tilde{q}_r\right) := \varphi\left(\tilde{q}_r + H_r x_{r,eq}\right) - \varphi\left(H_r x_{r,eq}\right) + \delta\tilde{q}_r$ and $\tilde{v}_r = v_r - v_{r,eq} - \delta\tilde{q}_r$. For the system at hand, it holds that $(A_{r,t}, B_r)$ is controllable, and $(A_{r,t}, C_r)$ is observable. Note that the first controller objective in 3.1 (stabilization) can now be formulated as the desire to stabilize the origin of (11) by the design of output-feedback controllers inducing the (feedback part of the) control input $\tilde{u}$. The latter is the topic of Section 4.

4. DESIGN OF OBSERVER-BASED OUTPUT-FEEDBACK CONTROLLERS

The control design strategy proposed here builds upon an observer-based controller for Lur'e-type systems with discontinuities as in [7, 41]. In these previous works, the controller and observer were designed for a drill-string model with a single flexibility mode and with the assumption on the availability of down-hole measurements, while in the current work, we adopt more realistic multi-modal drill-string models (Section 2) and develop controllers on the basis of surface measurements

DOI: 10.1002/rnc

only. Moreover, the conditions for controller synthesis as in [7] achieving *global* asymptotic stability, for the realistic drill-string model presented here, are infeasible for three reasons: firstly, the incorporation of multiple torsional flexibility modes of the drill-string, see Figure 3, secondly, the incorporation of a bit–rock interaction model based on field data, which shows a rather severe velocity-weakening effect, see Figure 2, and, thirdly, the restriction on the availability of only surface measurements. Therefore, we employ a controller synthesis strategy to design *locally* stabilizing controllers, and we show that such local stability properties suffice to mitigate stick–slip oscillations in realistic drilling scenarios. In Section 4.1, we propose the state-feedback controller, in Section 4.2, the observer design, and in Section 4.3, the resulting output-feedback control strategy, all including stability guarantees.

4.1. State-feedback controller design

In this section, we discuss the design of a state-feedback controller that stabilizes the origin $\xi_r = 0$ of the system (11). Stabilization of the origin of (11) corresponds to the desired operation of constant angular velocity of the drilling system, as discussed in 3.2. The control input is given by $\tilde{u} \in \mathbb{R}$, the input and output of the set-valued nonlinearity $\tilde{\varphi}_r$ are given by $\tilde{q}_r \in \mathbb{R}$, and $\tilde{v}_r \in \mathbb{R}$, respectively, and the system matrices are $A_{r,t} \in \mathbb{R}^{m_r \times m_r}$, $B_r \in \mathbb{R}^{m_r \times 1}$, $G_r \in \mathbb{R}^{m_r \times 1}$ and $H_r \in \mathbb{R}^{1 \times m_r}$. We introduce a linear static state-feedback law, where we take the 'measurement' (or observer) error $e := \xi_r - \hat{\xi}_r$ into account as follows:

$$\tilde{u} = K\hat{\xi}_r = K\left(\xi_r - e\right). \tag{12}$$

Herein, $K \in \mathbb{R}^{1 \times m_r}$ is the control gain matrix, and $\hat{\xi}_r$ the observer estimate of the state ξ_r; the observer will be treated in detail in Section 4.2. The resulting closed-loop system is described by the following differential inclusion:

$$\begin{aligned} \dot{\xi}_r &= \left(A_{r,t} + B_r K\right)\xi_r + G_r\tilde{v}_r - B_r K e \\ \tilde{q}_r &= H_r\xi_r \\ \tilde{v}_r &\in -\tilde{\varphi}_r\left(\tilde{q}_r\right). \end{aligned} \tag{13}$$

The transfer function $G_{cl}(s)$ from the input $\tilde{v}_r$ to the output $\tilde{q}_r$ of system (13) is given by $G_{cl}(s) = H_r(sI - (A_{r,t} + B_r K))^{-1}G_r,\ s \in \mathbb{C}$. Now, let us state the following assumption on the properties of the set-valued nonlinearity $\tilde{\varphi}_r(\tilde{q}_r)$. Hereto, we first define a set $\mathcal{S}_a$ for which $\tilde{\varphi}_r$ satisfies a particular sector condition: $\mathcal{S}_a := \{\tilde{q}_r \in \mathbb{R} | \tilde{q}_{r,a1} < \tilde{q}_r < \tilde{q}_{r,a2}\}$ with $\tilde{q}_{r,a1} < 0 < \tilde{q}_{r,a2}$.

Assumption 1
The set-valued nonlinearity $\tilde{\varphi}_r : \mathbb{R} \to \mathbb{R}$ satisfies the following conditions:

- $0 \in \tilde{\varphi}_r(0)$;
- $\tilde{\varphi}_r$ is continuously differentiable and bounded for all $\tilde{q}_r \in \mathcal{S}_a$;
- $\tilde{\varphi}$ locally satisfies the $[0, k]$ sector condition, with $k > 0$, in the sense that

$$\tilde{v}_r\left[\tilde{v}_r + k\tilde{q}_r\right] \leqslant 0 \quad \forall\ \tilde{v}_r \in -\tilde{\varphi}_r(\tilde{q}_r), \text{with } \tilde{q}_r \in \mathcal{S}_a. \tag{14}$$

Remark 1
The case where $\tilde{\varphi}_r$ is non-smooth or even discontinuous on the domain $\mathcal{S}_a$ can also be treated using the approach presented in [7]. However, this is not necessary for the application presented in this paper, because we pursue the design of controllers locally stabilizing a non-zero rotational velocity of the drill-string system.

The intended control goal is to render the closed-loop system (13) LISS with respect to the input e, as formalized in Definition 1, by a proper design of the controller gain K. We use the concept of a dynamic multiplier to transform the original system into a feedback interconnection of two passive systems. In Figure 4, a block diagram of the system including the dynamic multiplier with transfer function $M(s) = 1 + \gamma s,\ s \in \mathbb{C}$, is shown. Furthermore, the loop transformation gain $\frac{1}{k}$ is

DOI: 10.1002/rnc

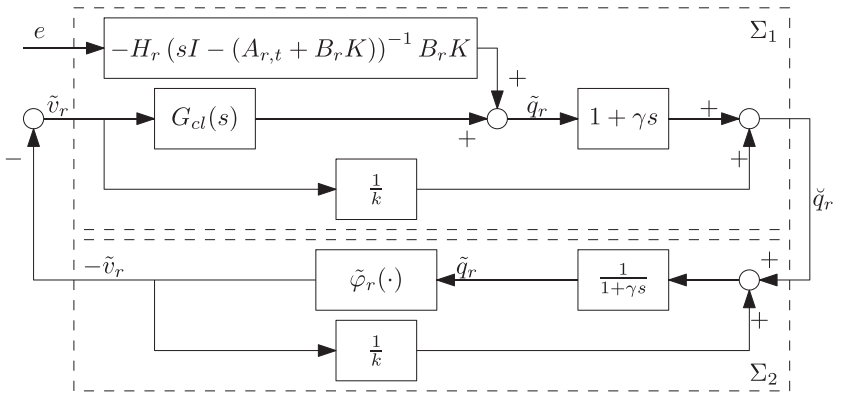

Figure 4. Schematic representation of system (13) after transformation using a dynamic multiplier.

included given the fact that the nonlinearity $\tilde{\varphi}_r(\cdot)$ belongs to the sector $[0, k]$. The linear system Σ_1 in Figure 4 can be written in state-space form as follows:

$$\Sigma_1 : \begin{cases} \dot{\xi}_r &= (A_{r,t} + B_r K)\,\xi_r + G_r \tilde{v}_r - B_r K e \\ \breve{q}_r &= \breve{H}_r \xi_r + \breve{D}_r \tilde{v}_r + \breve{Z}_r e \end{cases} \tag{15}$$

with $\breve{H}_r := H_r + \gamma H_r\,(A_{r,t} + B_r K)$, $\breve{D}_r := \frac{1}{k} + \gamma H_r G_r$ and $\breve{Z}_r := -\gamma H_r B_r K$. For system Σ_2 in Figure 4 we can write:

$$\Sigma_2 : \begin{cases} \dot{\tilde{q}}_r &= -\frac{1}{\gamma}\tilde{q}_r + \frac{1}{\gamma}\breve{q}_r - \frac{1}{\gamma k}\tilde{v}_r \\ \tilde{v}_r &\in -\tilde{\varphi}_r(\tilde{q}_r). \end{cases} \tag{16}$$

The following theorem states sufficient conditions under which system (13) is LISS with respect to input e.

Theorem 1
Consider system (13) and suppose that there exists a constant $\gamma > 0$ such that $\left(A_{r,t} + B_r K, G_r, \breve{H}_r, \breve{D}_r\right)$ is strictly passive. Then, system (13) is LISS, with respect to input e for any $\tilde{\varphi}_r(\cdot)$ satisfying Assumption 1.

Proof
The proof of Theorem 1 is given in Appendix A. □

4.2. Observer design

Next, an observer will be designed to construct an estimate of the states of system (11). Such a state estimate is needed because we only rely on surface measurements while, at the same time, aiming to employ the state-feedback controller of Section 4.1. The proposed observer design builds upon the result in [41]. We propose the following observer:

$$\begin{aligned} \dot{\hat{\xi}}_r &= (A_{r,t} - L C_r)\,\hat{\xi}_r + B_r \tilde{u} + G_r \hat{v}_r + L \tilde{y}_r \\ \hat{q}_r &= (H_r - N C_r)\,\hat{\xi}_r + N \tilde{y}_r \\ \hat{y}_r &= C_r \hat{\xi}_r \\ \hat{v}_r &\in -\tilde{\varphi}_r\,(\hat{q}_r)\,, \end{aligned} \tag{17}$$

with measured output $\tilde{y}_r = C_r \xi_r$ ($\tilde{y}_r \in \mathbb{R}^{k_r}$ and $C_r \in \mathbb{R}^{m_r \times k_r}$) and observer gain matrices $L \in \mathbb{R}^{m_r \times k_r}$ and $N \in \mathbb{R}^{1 \times k_r}$. Next, we state an additional assumption on the nonlinearity $\tilde{\varphi}_r(\cdot)$. Hereto, we first define the set $\mathcal{S}_b$ as $\mathcal{S}_b := \left\{\tilde{q}_r \in \mathbb{R} \middle| \tilde{q}_{r,b1} < \tilde{q}_r < \tilde{q}_{r,b2}\right\}$ with $\tilde{q}_{r,b1} < 0 < \tilde{q}_{r,b2}$, such that for all $\tilde{q}_r \in \mathcal{S}_b$, the following monotonicity property holds.

DOI: 10.1002/rnc

Assumption 2
The set-valued nonlinearity $\tilde{\varphi}_r : \mathbb{R} \to \mathbb{R}$ is such that $\tilde{\varphi}_r$ is monotone for all $\tilde{q}_r \in \mathcal{S}_b$, that is, for all $q_1 \in \mathcal{S}_b$ and $q_2 \in \mathcal{S}_b$ with $v_1 \in \tilde{\varphi}_r(q_1)$ and $v_2 \in \tilde{\varphi}_r(q_2)$, it holds that $(v_1 - v_2)(q_1 - q_2) \geqslant 0$.

The observer error dynamics (with the observer error defined as $e = \xi_r - \hat{\xi}_r$) can be written as

$$\begin{aligned} \dot{e} &= (A_{r,t} - LC_r)\, e + G_r\, (\tilde{v}_r - \hat{v}_r) \\ \tilde{v}_r &\in -\tilde{\varphi}_r(H_r \xi_r) \\ \hat{v}_r &\in -\tilde{\varphi}_r \left(H_r \hat{\xi}_r + N \left(\tilde{y}_r - C_r \hat{\xi}_r \right) \right). \end{aligned} \tag{18}$$

The following theorem provides sufficient conditions under which the origin $e = 0$ is a locally exponentially stable equilibrium point of the observer error dynamics (18). These conditions can be employed to constructively design the observer gains L and N.

Theorem 2
Consider system (11) and the observer (17) with $(A_{r,t} - LC_r, G_r, H_r - NC_r, 0)$ strictly passive and the matrix G_r being of full column rank. If it holds that

$$\|\xi_r(t)\| \leqslant \epsilon \frac{\tilde{q}_{r,b,min}}{\|H_r\|}, \quad \forall t \geqslant 0,$$

for some $\epsilon \in (0, 1)$ and $\tilde{q}_{r,b,min} := \min\left(\left|\tilde{q}_{r,b1}\right|, \left|\tilde{q}_{r,b2}\right|\right)$, then $e = 0$ is a locally exponentially stable equilibrium point of the observer error dynamics (18) for any $\tilde{\varphi}_r$ satisfying Assumptions 1 and 2. The region of attraction contains the set

$$\left\{ e \in \mathbb{R}^{m_r} \,\middle|\, \|e_0\| \leqslant (1 - \epsilon)\, \frac{\tilde{q}_{r,b,min}}{\|H_r - NC_r\|} \left(\frac{\lambda_{max}(P_o)}{\lambda_{min}(P_o)} \right)^{-\frac{1}{2}} \right\} \tag{19}$$

with the initial observer error $e(0) = e_0$. The matrix P_o in (19) results from the existence of $P_o = {P_o}^{\top} > 0$ and $Q_o = {Q_o}^{\top} > 0$ such that $P_o\,(A_{r,t} - LC_r) + (A_{r,t} - LC_r)\, P_o = -Q_o$ and ${G_r}^{\top} P_o = H_r - NC_r$, which is equivalent to the strict passivity of $(A_{r,t} - LC_r, G_r, H_r - NC_r, 0)$.

Proof
The proof of Theorem 2 is given in Appendix B. □

4.3. Output-feedback control design

The state-feedback controller and the observer from the previous sections together form an observer-based output-feedback controller. We use the estimated state $\hat{\xi}_r$ of the observer (17) in the feedback law (12) of system (13) and with the aforementioned Theorem 3, we prove local asymptotic stability of the equilibrium $(\xi_r, e) = (0, 0)$ of the interconnected system (13), (18), with $\hat{\xi}_r = \xi_r - e$.

Theorem 3
Consider system (13) and observer (17). Suppose the conditions in Theorem 1 are satisfied for system (13), and that the observer error dynamics in (18) satisfies the conditions in Theorem 2. Then, $(\xi_r, e) = (0, 0)$ is a locally asymptotically stable equilibrium point of the interconnected system (13), (18) for any $\tilde{\varphi}$ satisfying Assumptions 1 and 2.

Proof
The proof of Theorem 3 is given in Appendix C. □

5. A SIMULATION CASE STUDY

In this section, the observer-based output-feedback controller, as introduced in Section 4, will be applied to the reduced-order drill-string model presented in Section 2. To stabilize the desired

DOI: 10.1002/rnc

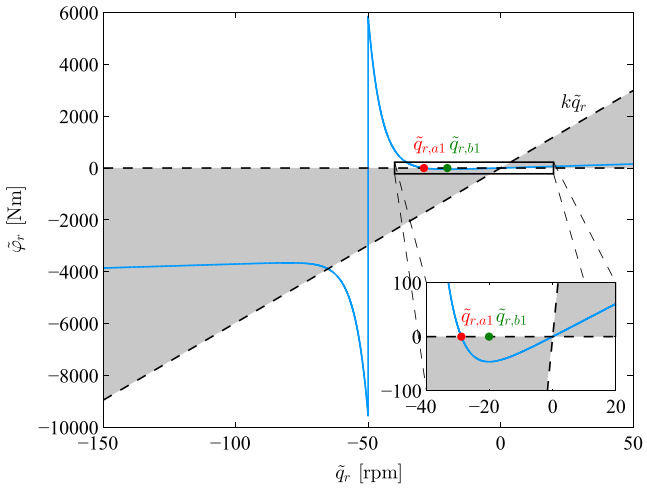

Figure 5. Transformed bit–rock interaction model $\tilde{\varphi}_r(\tilde{q}_r)$, satisfying the $[0, k]$-sector condition, with $k = 570$ Nms/rad. [Colour figure can be viewed at wileyonlinelibrary.com]

equilibrium $x_{r,eq}$ (corresponding to a desired angular velocity of 50 rpm in this case) of system (9), we have to design the controller gain K and the observer gains L and N to apply the control torque

$$u_t = u_c + K\hat{\xi}_r, \tag{20}$$

with u_c the constant feedforward torque as determined in Section 3.2 and $K\hat{\xi}_r$ the feedback torque based on the observer estimate $\hat{\xi}_r$.

For the design of the controller and observer gains, we consider the system in perturbation states (11). Moreover, a linear loop transformation is employed such that the transformed set-valued nonlinearity satisfies the conditions in Assumptions 1 and 2. To illustrate both aspects, the transformed nonlinearity $\tilde{\varphi}_r(\tilde{q}_r)$, with $\delta = 29.2$ Nms/rad, is shown in Figure 5. This figure shows that $\tilde{\varphi}_r(\tilde{q}_r)$ belongs locally to the sector $[0, k]$ with $k = 570$ Nms/rad. We have also indicated the point $\tilde{q}_{r,a1} = -28.9$ rpm for which it holds that for $\tilde{q}_{r,a1} < \tilde{q}_r < \tilde{q}_{r,a2}$, the sector condition (14) is satisfied ($\tilde{q}_{r,a2}$ can be chosen arbitrarily large in this case) and hence Assumption 1 is satisfied. Moreover, the point $\tilde{q}_{r,b1} = -20.1$ rpm such that for $\tilde{q}_{r,b1} < \tilde{q}_r < \tilde{q}_{r,b2}$, it holds that $\tilde{\varphi}_r$ is monotonically increasing ($\tilde{q}_{r,b2}$ can also be chosen arbitrarily large in this case) and hence Assumption 2 is satisfied. The sector, and therewith the parameters δ and k, is chosen such that a controller can be designed which has, on the one hand, robustness with respect to uncertainty in the bit–rock interaction (i.e., a large sector) and, on the other hand, the control action is limited, i.e., control gains that result in feasible control torques u_t ($= T_{td}$) for a typical top drive.

The controller and observer gains are designed according to the conditions given in Theorems 1 and 2, respectively. The results are obtained by using SeDuMi 1.3 [42], a linear matrix inequality (LMI) solver and the YALMIP interface [43]. The designed controller and observer gains are given by

$$K = \begin{bmatrix} -276.9 & 201.7 & -228.1 & -481.4 & 370.6 & 192.1 & 549.1 & 272.7 & 68.79 \end{bmatrix},$$
$$L = \begin{bmatrix} 40.14 & 64.19 & 87.96 & -187.3 & -239.9 & 183.5 & 428.0 & 347.5 & -6.515 \end{bmatrix}^\top, \; N = 0.502.$$

In this case study, we introduce a so-called startup scenario, which is based on practical startup procedures for drilling rigs. This startup scenario is important because of the locally stabilizing nature of the designed controller. The startup scenario ensures that the angular velocity and WOB are gradually increased to avoid transient oscillations as is also common in practical drilling operations. In the startup scenario, the drill-string is first accelerated to a low constant rotational velocity with the bit above the formation (off bottom) and, subsequently, the angular velocity and WOB are increased to the desired operating conditions. The startup scenario is built up as follows:

DOI: 10.1002/rnc

(1) Start with zero WOB, which on a model level is reflected by the absence of a velocity-weakening effect in the bit–rock interaction model. Moreover, an industrial PI-controller, see (23) below for details, is used to operate at relatively low velocity and build up torque in the drill-string to overcome static torques owing to drag in the time window $0 < t < 50$ s;
(2) The controller (20) is activated at $t = 50$ s, and the reference angular velocity is slowly increased until the desired operating velocity (ω_{eq}) is reached (in the time window $50 \leqslant t < 110$ s). At the same time, we emulate that the WOB slowly increases (by adaptation of the bit–rock interaction model as in (21), (22) below) to engage the drilling process in order to generate the nominal operating condition in both the angular velocity and the WOB (and hence bit torque).

The change in the WOB is modelled as a change in the TOB T_{bit}. In particular, the bit–rock interaction model in (7) is scaled using a scaling factor $\alpha(t)$ according to

$$T_{bit}(t) = \mathrm{Sign}(\omega_{bit}) \left(T_{ini} + \alpha(t) \left(T_d - T_{ini} + (T_s - T_d)\, e^{-\frac{30}{N_d \pi} |\omega_{bit}|} \right) \right), \tag{21}$$

where

$$\alpha(t) = \begin{cases} 0, & t_0 \leqslant t \leqslant t_1 \\ \frac{t - t_1}{t_2 - t_1}, & t_1 < t < t_2 \\ 1, & t \geqslant t_2 \end{cases} \tag{22}$$

with $t_1 = 50$ and $t_2 = 110$ in this case and T_{ini} is the amount of resisting torque that is still present at the bit–rock interface, even when the bit is off bottom (e.g., owing to drilling mud and interactions with the bore hole).

Before we show the simulation results of the designed output-feedback controller, we will show a simulation result of the reduced-order drill-string system in closed loop with an existing industrial controller (based on [5]). The result of the simulation of the reduced-order model in closed loop with the industrial (SoftTorque) controller is shown in Figure 6. This controller is a properly tuned active damping system (in particular PI-control based on feedback of the angular velocity of the top drive). This controller aims at damping the first torsional mode of the drill-string dynamics, on

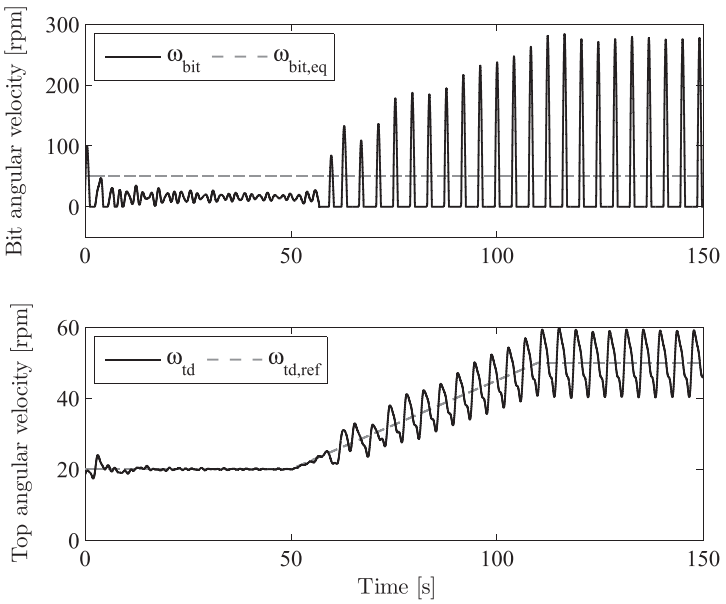

Figure 6. Simulation result of the reduced-order model (9) with an existing industrial (SoftTorque) controller in the startup scenario.

DOI: 10.1002/rnc

the basis the error $e_y := \omega_{td,ref} - \omega_{td}$ between the measured top drive velocity $y = \omega_{td}$ and the reference angular velocity $\omega_{td,ref}$. The controller is given in the Laplace domain by

$$\tilde{u}(s) = \left(c_t + \frac{k_t}{s}\right) e_y(s) \tag{23}$$

with $c_t = 1829$ and $k_t = 1177$ (based on [39]) such that damping of the first torsional flexibility mode is obtained. The second plot of Figure 6 shows the top drive velocity (ω_{td}) along with the reference velocity $\omega_{td,ref}$ that starts at a velocity of 20 rpm and is gradually increased to the desired equilibrium velocity, ω_{eq}, of 50 rpm. From the bit response, in the upper plot of Figure 6, we can clearly recognize stick–slip oscillations. The increasing amplitude of the oscillations in the top drive velocity demonstrates that these vibrations arise when the WOB (and hence TOB) is increased ($50 \leqslant t < 110$ s). This increase in TOB is modelled as explicated in (21), (22) and therewith induces an increasing amount of velocity-weakening in the bit–rock interaction. Clearly, the fully engaged bit–rock interaction law has a destabilizing effect and the SoftTorque controller is no longer able to stabilize the desired equilibrium and eventually stick–slip oscillations appear.

For the output-feedback controller proposed in Section 4, we immediately activate (at $t = 0$) the observer to obtain the state estimate $\hat{\xi}_r$; however, this estimate is not used by the industrial PI-controller in the first 50 s (because this controller only uses the top drive velocity as a measured output). When the state-feedback controller is switched on at $t = 50$, it uses the state estimate $\hat{\xi}_r$, the latter of which is obtained on the basis of the surface measurement ω_{td} only. Figure 7 shows a simulation result of the closed-loop system with this output-feedback controller, where we used the same initial conditions $\xi_{r,0}$ and startup scenario as for the previous simulation (6).

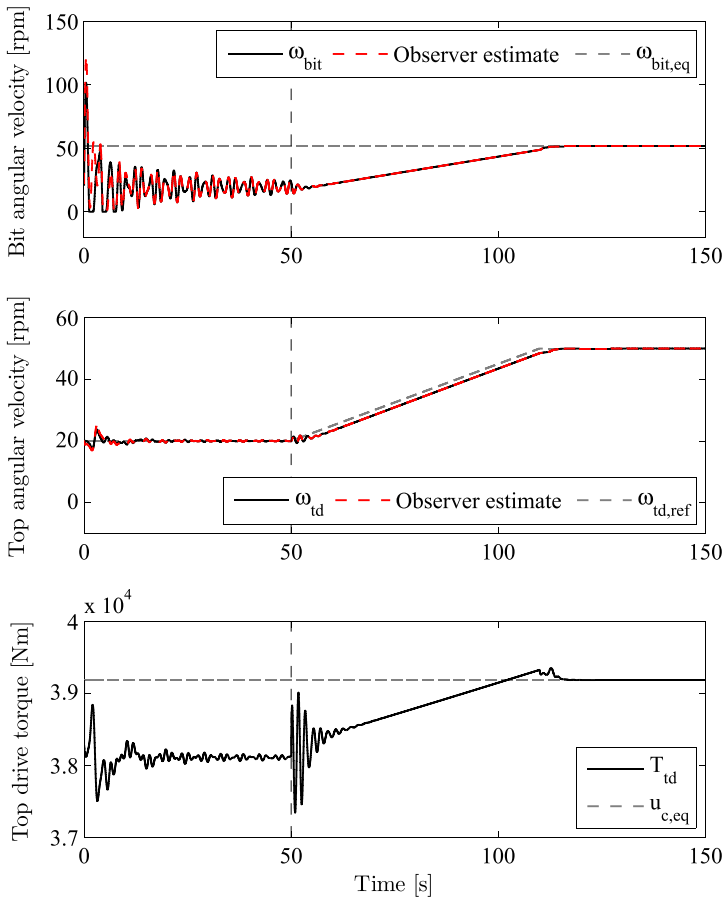

Figure 7. Simulation result of the reduced-order model with the designed output-feedback controller in the startup scenario. [Colour figure can be viewed at wileyonlinelibrary.com]

DOI: 10.1002/rnc

Furthermore, the initial states for the observer $\hat{\xi}_{r,0}$ have a 10% offset from the initial states $\xi_{r,0}$. It can be seen that after some transient behavior, the observer estimates converge to the actual states within approximately 5 s. After 50 s, the output-feedback controller is turned on and the WOB and desired velocity are increased. The simulation results show that the top drive and bit velocity converge to their equilibrium value and stick–slip oscillations are avoided. The equilibrium velocity of the bit $\omega_{bit,eq} := H_r x_{r,eq} \approx 47$ rpm is slightly lower than the equilibrium velocity of the top drive $\omega_{td,eq} = \omega_{eq} = 50$ rpm. This small mismatch is a consequence of the model reduction employed to construct the reduced-order model employed in the observer, as mentioned in 3.2. It is also important to mention that the control action (T_{td}) is limited as can be seen in the top drive torque in the bottom plot. More precisely, the control action (T_{td}) is well within the capabilities of the top drive in terms of torque amplitude and frequency; hence, the risk of stalling the bit as a result of a top drive overload is very low. This is a key aspect for a field application.

Most importantly, it can be concluded that the stick–slip vibrations are eliminated with the designed controller in a realistic drilling scenario in which a state-of-the-art industrial controller can not avoid such undesired oscillations. Besides (local) asymptotic stability of the desired setpoint, the controller is designed to obtain robustness with respect to uncertainty in the bit–rock interaction. As mentioned in Section 2.1, the bit-mobility can be used to investigate the sensitivity for disturbances induced by the bit–rock interaction. Therefore, we would like to analyze whether indeed damping of the resonance modes in the bit-mobility is obtained with the designed observer-based controller. To do so, we use a linearized approximation of the reduced-order nonlinear closed-loop system to determine the closed-loop bit-mobility. The approximated closed-loop system in perturbation coordinates and linearized around $(\xi_r, \hat{\xi}_r) = (0, 0)$ is given by

$$\begin{aligned}
\dot{\xi}_r &= \left(A_r - G_r H_r \left.\frac{\partial \varphi}{\partial q_r}\right|_{\xi_r=0,\hat{\xi}_r=0} \right) \xi_r + B_r K \hat{\xi}_r \\
\dot{\hat{\xi}}_r &= \left(A_r - LC_r + B_r K - G_r \left(H_r - NC_r\right) \left.\frac{\partial \varphi}{\partial \hat{q}_r}\right|_{\xi_r=0,\hat{\xi}_r=0} \right) \hat{\xi}_r \\
&\quad + \left(LC_r - G_r N C_r \left.\frac{\partial \varphi}{\partial \hat{q}_r}\right|_{\xi_r=0,\hat{\xi}_r=0} \right) \xi_r .
\end{aligned} \tag{24}$$

On the basis of this linearized closed-loop system, we can determine the closed-loop bit-mobility as shown in Figure 8. For the sake of comparison, we have also shown closed-loop bit-mobility of the system with the industrial SoftTorque controller. It can be observed that with the industrial controller only the first torsional flexibility mode is damped, which can be an explanation for the fact that the drill-string system still exhibits stick–slip oscillations when controlled by the SoftTorque controller. The designed observer-based controller, on the other hand, clearly achieves damping of all three flexibility modes of the reduced-order model. Clearly, damping of multiple flexibility modes in the bit-mobility can be achieved with the proposed controller design methodology, thereby enhancing its capability to mitigate stick–slip oscillations.

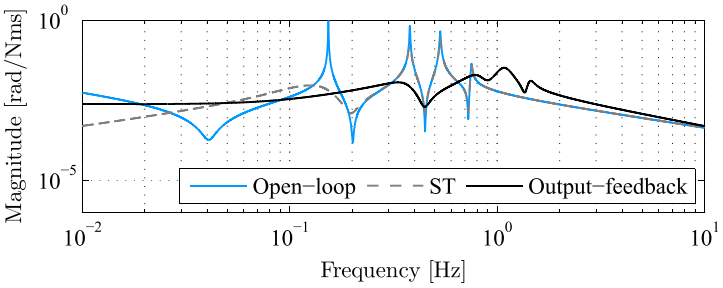

Figure 8. Closed-loop bit-mobility of the linearized reduced-order model, that is, the frequency response function from bit torque T_{bit} to bit velocity ω_{bit} for the linearized system (24). [Colour figure can be viewed at wileyonlinelibrary.com]

DOI: 10.1002/rnc

6. CONTROLLER DESIGN FOR THE 18-DOF MODEL

The application of the controller to the 18-DOF drilling system dynamics (8) is investigated in this section to establish the robustness of the controller for ' unmodelled' dynamics (owing to the differences between the reduced-order model and the 18-DOF FEM model). In the previous sections, the controller design strategy is applied to a reduced-order model of the drill-string dynamics. Stability conditions to guarantee (local) asymptotic stability are derived, and simulation results are presented to illustrate that the desired velocity can indeed be stabilized, thereby avoiding stick–slip oscillations. The purpose of the reduced-order model is to reduce the controller complexity (in particular of the observer), such that the LMI-based design of the state-feedback controller and observer are feasible. Additionally, a controller of limited order is also favorable for implementation reasons. However, in practice, the plant (i.e., the drilling system) of course exhibits richer dynamics than the reduced-order model, e.g., Figure 3. Therefore, the simulation results and stability analysis of the controller applied to the 18-DOF drill-string model, as presented in this section, are important to investigate the practical relevance of the developed control strategy.

The closed-loop system, consisting of the 18-DOF finite-element model of the drill-string dynamics and the observer-based output-feedback controller based on the reduced-order model, is given by the drill-string dynamics (8), the observer, on the basis of the reduced-order model:

$$\begin{aligned}
\dot{\hat{x}}_r &= A_r\hat{x}_r + B_r u_t + G_r\hat{v}_r + G_{2,r}\hat{v}_{2,r} + L\,(y - \hat{y}_r)\\
\hat{q}_r &= H_r\hat{x}_r + N\,(y - \hat{y}_r)\\
\hat{q}_{2,r} &= H_{2,r}\hat{x}_r\\
\hat{y}_r &= C_r\hat{x}_r\\
\hat{v}_r &\in -\varphi(\hat{q}_r)\\
\hat{v}_{2,r} &\in -\phi(\hat{q}_{2,r})
\end{aligned} \tag{25}$$

and the state-feedback controller $\tilde{u} = K\hat{\xi}_r = K\left(\hat{x}_r - x_{r,eq}\right)$.

As mentioned before, only the top drive angular velocity measurement is used and the measured output is given by $y = Cx = \omega_{td}$. The designed controller and observer gains for the closed-loop system (8) and (25), with the top drive angular velocity measurement only, are given by

$$\begin{aligned}
K &= \left[\,-276.9\ 201.7\ -228.1\ -481.4\ 370.6\ 192.1\ 549.1\ 272.7\ 68.79\,\right],\\
L &= \left[\,44.26\ 41.77\ 27.17\ -72.56\ -105.6\ 84.30\ 171.6\ 61.88\ 43.36\,\right]^{\top},\ N = 0.414.
\end{aligned} \tag{26}$$

The controller gains are equal to the controller gains designed for the reduced-order model in Section 5, the observer has been re-tuned (by changing the sector for the observer to $[0, k^*]$ with $k^* = 62$ Nms/rad). Owing to the smaller sector (for the observer only), the robustness with respect to uncertainty in the bit–rock interaction decreased; however, owing to the decreased observer gains in L and N, the robustness with respect to the model mismatch owing to reduction increased, which is beneficial for the (reduced-order) observer when applied to the 18-DOF model. With the observer gains L and N as designed in Section 5 (for the reduced-order model), the observer estimates show large transient oscillations and, therefore, re-tuning of the observer gains is necessary for application of the observer to the 18-DOF model.

A simulation result of the designed controller applied to the 18-DOF drill-string model is shown in Figure 9. For comparison, also the response of the system in closed-loop with the SoftTorque controller (indicated by the subscript ST) is shown. In the first 50 s, in both strategies, the same controller is used (as explained for the startup scenario); after 50 s, the observer-based controller is switched on while for the industrial controller the same controller is used for the whole time range. Between 50 and 110 s, the TOB and desired velocity are again changed according to the startup scenario to obtain the desired operating conditions. This simulation shows that the observer-based output-feedback controller clearly stabilizes the desired setpoint of 50 rpm, while the industrial controller does not stabilize the equilibrium, resulting in stick–slip oscillations at the bit.

DOI: 10.1002/rnc

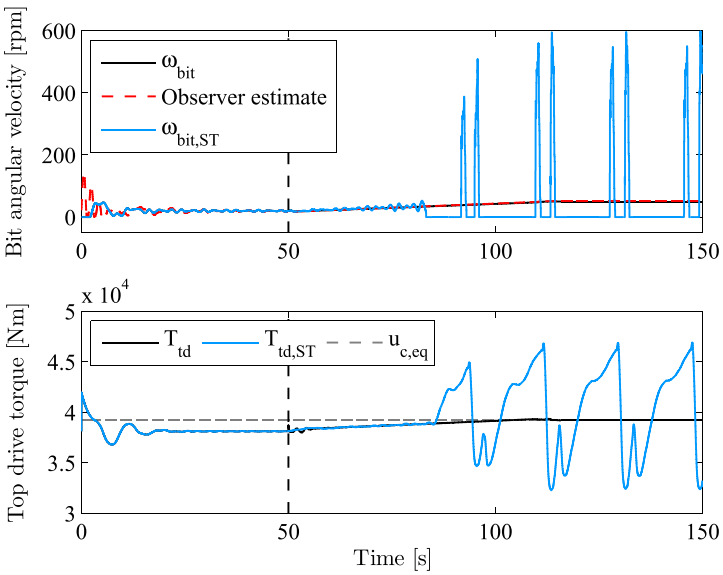

Figure 9. Simulation result of both the industrial (SoftTorque) controller and the designed observer-based output-feedback controller applied to the 18-DOF drill-string system. [Colour figure can be viewed at wileyonlinelibrary.com]

So as to conclude, the simulation result in Figure 9 shows that the controller is robust for the model mismatch introduced by the reduction procedure. This is an important property for the practical implementation of the proposed controller design strategy. In Section 6.1, a stability analysis based on linearization is performed for the closed-loop system investigated in this section. In Section 7, several other robustness aspects are investigated by means of simulation studies.

6.1. Stability analysis

The stability conditions, as presented in Section 4, apply to a closed-loop system where the controller and observer are designed for and applied to the same plant. For the application of the reduced-order controller and observer to a higher-order model (or real drilling system), stability is not necessarily guaranteed owing to model mismatches. However, simulation results presented earlier show that the reduced-order controller and observer can still (locally) stabilize the desired equilibrium of the high-order finite-element model. So as to further investigate the stability of the equilibrium point of the closed-loop nonlinear system, the closed-loop system is linearized around this equilibrium point and stability of the linearized system is investigated. The linearized closed-loop system, in perturbation coordinates, and linearized around $(\xi, \hat{\xi}_r) = (0, 0)$ is given by

$$\begin{aligned}
\dot{\xi} &= \left(A - GH \left.\frac{\partial \varphi}{\partial q}\right|_{\xi=0,\hat{\xi}_r=0} \right) \xi + BK\hat{\xi}_r \\
\dot{\hat{\xi}}_r &= \left(A_r - LC_r + B_r K - G_r \left(H_r - NC_r\right) \left.\frac{\partial \varphi}{\partial \hat{q}_r}\right|_{\xi=0,\hat{\xi}_r=0} \right) \hat{\xi}_r \\
&\quad + \left(LC - G_r NC \left.\frac{\partial \varphi}{\partial \hat{q}_r}\right|_{\xi=0,\hat{\xi}_r=0} \right) \xi.
\end{aligned} \tag{27}$$

As can be seen from this equation, both the nonlinearity in the plant and the nonlinearity in the observer are linearized. For a desired velocity of 50 rpm, the real value of the right-most pole of the system matrix of the linear time-invariant system dynamics in (27) equals $\max(\mathrm{Re}(\lambda_i)) = -0.015$; hence, the desired setpoint is locally (exponentially) stable, which is in accordance to the simulation results shown in Figure 9. Surprisingly, the equilibrium of the closed-loop with the industrial controller used for the simulation in the same figure is also stable ($\max(\mathrm{Re}(\lambda_i)) = -0.022$). As

DOI: 10.1002/rnc

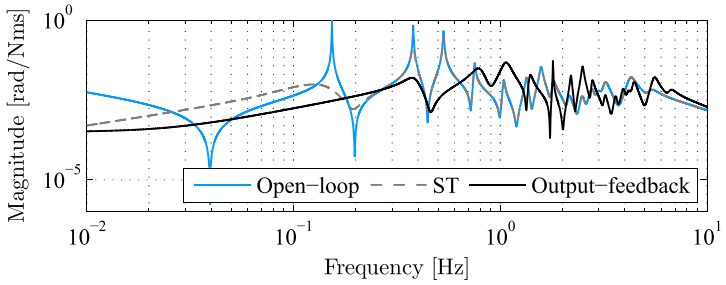

Figure 10. Closed-loop bit-mobility, i.e. the frequency response function from bit torque T_{bit} to bit velocity ω_{bit} for the linearized system (27). [Colour figure can be viewed at wileyonlinelibrary.com]

we have observed in the simulation, this controller failed to stabilize the desired velocity. The latter fact can be explained as follows. The controller does not only need to guarantee (local) stability, it also needs to be robust with respect to, for example, disturbances (e.g. induced by the build-up of reference velocity and TOB) and model mismatches to ensure mitigation of stick–slip oscillations. Investigation of the closed-loop system has revealed that robustness with respect to the bit–rock interaction is particularly important for the stability of the desired setpoint of the nonlinear closed-loop system.

Because the velocity-weakening effect in the bit–rock interaction has a destabilizing effect, a controller should be designed such that the robustness with respect to this negative damping effect is 'optimized'. An indication of such robustness property is given by the closed-loop bit-mobility function. The open-loop bit-mobility function of the drill-string system is defined by G_{cl} and shown in Figure 3(c). Using the linearized system (27), we can also investigate the closed-loop bit-mobility transfer function. In Figure 10, the magnitude of the closed-loop bit-mobility of the system with the observer-based controller and the industrial controller are shown and compared with the open-loop bit-mobility. For the industrial controller, only the first mode is damped, while higher flexibility modes are still present. These undamped higher flexibility modes (especially those at 0.38 and 0.53 Hz) can be related to the fact that stick–slip oscillations are still present when the SoftTorque controller is applied. The proposed controller design strategy clearly achieves damping of multiple flexibility modes. From Figure 10, it can be seen that the first three modes are well-damped by the observer-based output-feedback controller, where these first three modes are the dominant flexibility modes in the open-loop bit-mobility. This confirms that, with the proposed controller design strategy, it is indeed possible to damp multiple flexibility modes. Owing to the achieved damping of the bit-mobility, larger variations in the bit angular velocity are allowed to occur; that is, the region of attraction in terms of the bit-angular velocity is increased. In other words, the system robustness in terms of stick–slip mitigation has been improved.

7. ROBUSTNESS ANALYSIS OF THE CLOSED-LOOP SYSTEM

The simulation studies presented in this section are all performed using the 18-DOF model, that is, simulation case-studies for the closed-loop system consisting of the finite-element model for the drill-string and the observer-based output-feedback controller based on the reduced-order model. In the previous section, the simulation has been performed under 'ideal' conditions, that is, without disturbances and/or changing operating conditions in terms of desired angular velocity, increasing length of the drill-string and changing bit–rock interaction. These robustness aspects are key in the scope of practical application of the proposed controller design strategy. In the field, the prognosis of the lithology (rock types) and expected thicknesses of each lithology are usually given. Different lithologies are related to the required robustness with respect to uncertainties in the bit–rock interaction. Different formation thickness is related to the required robustness with respect to the varied length of the drill-string. These scenarios can be used as a part of the pre-commissioning workflow to test the robustness of the controller prior to field applications. In this section, simulation results are presented where these effects are taken into account. All these results are obtained for a

DOI: 10.1002/rnc

closed-loop system with the 18-DOF FEM model, and the reduced-order controller with the gains given in (26).

7.1. *Different operating velocity*

The designed controller (Section 6) is synthesized for a desired angular velocity of 50 rpm. This controller is designed such that, on the one hand, the robustness with respect to the bit–rock interaction is improved and, on the other hand, the control action is limited, that is, feasible for a typical top drive. This balance is achieved by tuning the sector bound k, and the slope of the transformed nonlinearity $\tilde{\varphi}_r$ around the desired setpoint (determined by δ). On the basis of an analysis of the pole locations of the linearized drill-string dynamics (27), the desired equilibrium of the 18-DOF model with output-feedback controller is found to be locally asymptotically stable for velocities $\omega_{eq} \geqslant 31.9$ rpm. For the system with SoftTorque, this lower limit is approximately 40 rpm. We note that these velocities indicate a theoretical lower limit and the lowest velocity for which stick–slip oscillations can be avoided will be higher. In practical situations, such as the startup scenario, we have seen that with the SoftTorque controller stick–slip oscillations already appeared for a desired angular velocity of 50 rpm. For the system with the nonlinear output-feedback controller, the minimum velocity that can be stabilized in simulations using the startup procedure is approximately 41.5 rpm. Clearly, the proposed control strategy significantly widens the operational envelope of the drilling system.

7.2. *Changing bit–rock interaction model*

In practice, it is difficult to obtain an accurate model for the bit–rock interaction; moreover, the bit–rock interaction characteristic is prone to changes during the drilling process owing to changing formation characteristics and bit wear. Robustness with respect to uncertainty in the bit–rock interaction is key in practice and is obtained by enlarging the sector k for the bit–rock interaction in the controller synthesis. In this section, a simulation result is shown to illustrate the variations in the bit–rock interaction that the proposed controller can cope with.

Recall the nominal parameter values for the bit–rock interaction model, that is, $T_s = 7700$ Nm, $T_d = 1700$ Nm and $N_d = 5$ rpm. These values are used in the controller synthesis and are also used in the observer. Owing to changing conditions, the actual bit–rock interaction, acting on the plant, may change. In the simulation study presented here, both the torque level and the decrease rate of the bit–rock interaction are changed. The parameters for the adapted bit–rock interaction model are given by $T_s^c = T_s + 500$, $T_d^c = T_d + 500$ and $N_d^c = N_d + 1$. This leads to a less severe velocity-weakening effect and therefore more negative damping at higher velocities and a (torque-level) offset between the two bit–rock interaction models. The nominal and adapted bit–rock interaction model are shown in the left plot in Figure 11. The plot on the right-hand side shows the equivalent transformed representation of both bit–rock interaction models. It can be seen that both bit–rock interaction models (locally) satisfy the $[0, k]$ sector condition. It has to be mentioned that the increase of the torque level (at the setpoint angular velocity) is compensated by the feedforward torque, that is, the plant uses a higher (constant) feedforward torque than the observer. This is a reasonable assumption from a practical point of view, because the torque necessary to rotate the drill-string in steady-state can be determined from measurements while drilling.

The simulation result with the changed bit–rock interaction model is shown in Figure 12. It takes about 25 s before the states of the observer have converged to the actual states. When the observer-based controller is switched on after 50 s, the desired setpoint is stabilized and stick–slip oscillations have been mitigated. Moreover, the difference between the torque for the plant and the observer can be observed clearly in the bottom plot. As mentioned before, this difference is the (constant) difference between the actual feedforward torque and the observer feedforward torque that is based on the nominal bit–rock interaction.

So as to conclude, with the designed observer-based output-feedback controller robustness with respect to uncertainty in the nominal level of the bit–rock interaction, as well as, in the slope of the nonlinearity, has been obtained.

DOI: 10.1002/rnc

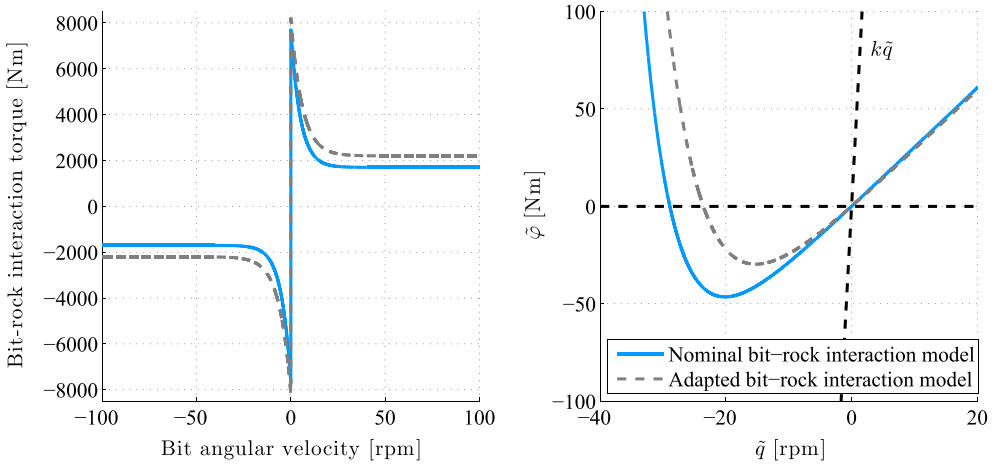

Figure 11. Nominal and adapted bit–rock interaction model, and a zoom plot of its equivalent transformed representations to indicate the sector bounds. [Colour figure can be viewed at wileyonlinelibrary.com]

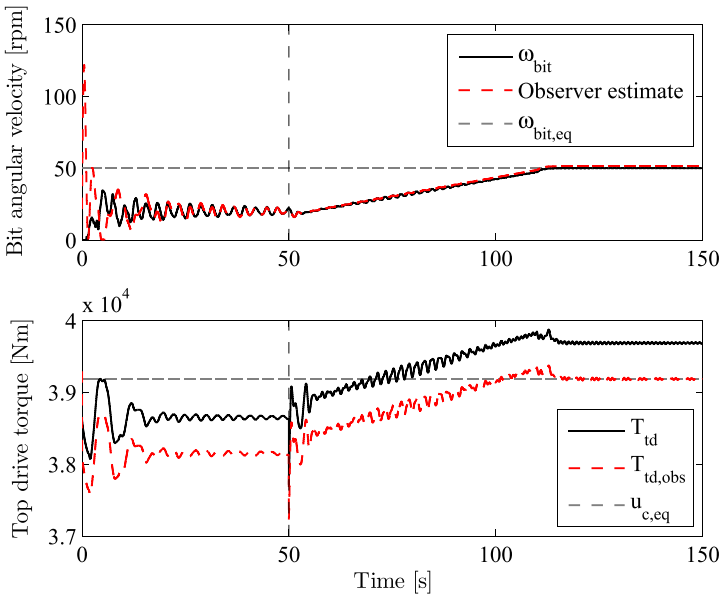

Figure 12. Simulation result of the closed-loop system with a changed bit–rock interaction for the plant model. [Colour figure can be viewed at wileyonlinelibrary.com]

7.3. Changing length of the drill-string

Another important aspect in the control of drilling systems is the change of length of the drill-string while drilling. Current controllers need to be re-tuned during the drilling operation, and this re-tuning is prone to errors, resulting in wrong controller settings and possibly failing to mitigate stick–slip oscillations owing to tuning errors. Therefore, it is of practical importance to reduce the need for re-tuning owing to length changes in the drill-string. In this section, the plant model (8) is changed such that the dynamics of the plant correspond to a drill-string of different length. The controller remains the same, and the observer is always based on the nominal reduced-order model (9).

In this analysis, it is assumed that several new stands, of three drill pipes of 9-m length each, are added to the drill-string (i.e., 27 m of length is added to the drill-string with each stand). In practical situations, the current industrial controller needs to be re-tuned every stand and sometimes even after one or two added drill pipes. The results of the analysis of the linearized closed-loop system with different lengths are shown in Figure 13. The real value of the right-most eigenvalue,

DOI: 10.1002/rnc

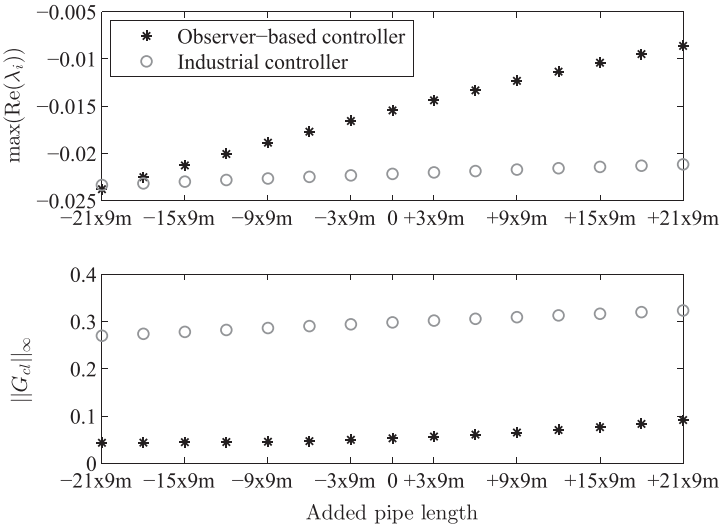

Figure 13. Location of the right-most eigenvalue of the closed-loop system and $\mathcal{H}_\infty$-norm of the bit-mobility as function of added pipe length to the drill-string.

associated with the linearized models, is shown as function of changing length compared with the nominal model. The right-most eigenvalue of the nominal model (indicated by 0 on the horizontal axis) lies in the LHP as shown in Section 6.1. When the length of the drill-string is decreased the right-most eigenvalue moves further into the LHP, while for an increase of length, the right-most eigenvalue moves towards the imaginary axis. The same holds for the closed-loop system induced by the industrial controller (albeit more slowly). However, as mentioned before, the location of the eigenvalue is not the only important factor. Therefore, also the $\mathcal{H}_\infty$-norm[§] of the bit-mobility (G_{cl}) is shown in Figure 13. Recall that the bit-mobility is related to the robustness with respect to the bit–rock interaction. The $\mathcal{H}_\infty$-norm of the closed-loop bit-mobility with the observer-based controller is approximately a factor five lower than the $\mathcal{H}_\infty$-norm of G_{cl} with the industrial controller, as was also visible in the bit-mobility plot (10) for the nominal case. The latter fact indicates that the system with the observer-based controller is more robust with respect variations in the bit–rock interaction, also for changing drill-string lengths.

Simulations (using the start-up scenario) with different plant models show that the observer-based controller is able to stabilize the desired setpoint for a drill-string model with a maximum of 39 pipe sections (i.e., 351 m) added to the nominal model, while the industrial controller is even unable to stabilize the desired setpoint of the nominal model as shown in Figure 9. It can be concluded that a significant increase in robustness with respect to increasing drill-string length is obtained compared with the industrial controller.

8. DISCUSSION

In this work, a nonlinear observer-based output-feedback control strategy is proposed to eliminate torsional stick–slip vibrations in drilling systems. Particular benefits of the proposed approach with respect to existing controllers are, firstly, the fact that a realistic multi-modal model of the drill-string dynamics is taken into account, secondly, that severe velocity-weakening (and uncertainty) in the bit–rock interaction is taken into account, thirdly, that only surface measurements are employed. Additionally, a guarantee for (local) asymptotic stability of the closed-loop reduced-order system is given for bit–rock interaction laws lying within a certain sector (which is beneficial as the bit–rock interaction is subject to uncertainty in practice). In supporting the controller synthesis, a reduced-order model is used, on the basis of a high-fidelity finite-element model for the drill-string dynamics.

[§]The $\mathcal{H}_\infty$-norm of a transfer function $H(s)$ is given by $\|H(s)\|_\infty := \sup_{\omega\in\mathbb{R}} (H(j\omega))$.

DOI: 10.1002/rnc

The reduced-order model is constructed such that it captures the dominant dynamics (flexibility modes) of the original system. Simulation studies show that the controller design strategy successfully eliminates stick–slip oscillations when applied to a realistic drill-string model in representative drilling scenarios for which an industrial SoftTorque controller is unable to do so.

Robustness of the closed-loop drill-string system with respect to several practical aspects is investigated by means of simulation studies. These studies show that the closed-loop system with the proposed controller is robust for the model mismatch introduced by the reduction procedure is able to operate for different angular velocity setpoints and is robust with respect to changes in the bit–rock interaction and length of the drill-string. Under all the imposed operating conditions, the controller is able to stabilize the desired angular velocity and therefore stick–slip vibrations are eliminated. These results show that a significant increase in the operating envelope can be achieved by using the proposed controller design methodology compared with currently used industrial controllers.

APPENDIX A: PROOF OF THEOREM 1

We will provide a concise proof (employing the results in [7]) while focussing on the local aspect of the stability properties certified by Theorem 1. Consider the following LISS Lyapunov function candidate:

$$V(\xi_r) = V_1(\xi_r) + V_2(\tilde{q}_r) \tag{28}$$

with $\tilde{q}_r = H_r \xi_r$ and

$$V_1(\xi_r) = \frac{1}{2} {\xi_r}^\top P \xi_r, \quad P = P^\top > 0, \tag{29}$$

$$V_2(\tilde{q}_r) = \gamma \int_0^{\tilde{q}_r} \tilde{\varphi}_r(\sigma) \mathrm{d}\sigma. \tag{30}$$

Note that $V_2(\tilde{q}_r)$ is continuously differentiable on the domain $\mathcal{S}_a \subset \mathbb{R}$ that contains $\tilde{q}_r = 0$. We will show that the function V satisfies the following bounds

$$\psi_1(\|\xi_r\|) \leqslant V(\xi_r) \leqslant \psi_2(\|\xi_r\|), \tag{31}$$

where ψ_1 and ψ_2 are class $\mathcal{K}_\infty$-functions. To do so, note that $V_2(\tilde{q}_r) \geqslant 0, \ \forall \tilde{q}_r \in \mathcal{S}_a$ since $\tilde{\varphi}_r$ belongs locally to $[0, k]$, with $k > 0$. Furthermore, we know that

$$\frac{1}{2}\lambda_{min}(P) \|\xi_r\|^2 \leqslant V_1(\xi_r) \leqslant \frac{1}{2}\lambda_{max}(P) \|\xi_r\|^2 . \tag{32}$$

Thus,

$$V(\xi_r) \geqslant \psi_1(\|\xi_r\|) := \frac{1}{2}\lambda_{min}(P) \|\xi_r\|^2 . \tag{33}$$

By using the sector condition (14), an upper bound for V_2 can be derived:

$$V_2(\tilde{q}_r) \leqslant \gamma \int_0^{|\tilde{q}_r|} |\tilde{\varphi}_r(\tilde{q}_r)| \, \mathrm{d}\sigma \leqslant \frac{\gamma k}{2} \|H_r\|^2 \|\xi_r\|^2 \tag{34}$$

Therefore,

$$V(\xi_r) \leqslant \psi_2(\|\xi_r\|) := \frac{1}{2}\lambda_{max}(P) \|\xi_r\|^2 + \frac{\gamma k}{2} \|H_r\|^2 \|\xi_r\|^2 . \tag{35}$$

Moreover, it can be shown (see [7]) that there exists a $\varepsilon > 0$ such that the time derivative of V along the trajectories satisfies

DOI: 10.1002/rnc

$$\dot{V} < -\psi_3(\|\xi_r\|) \quad \text{if } \|\xi_r\| \geqslant \chi(\|e\|) \tag{36}$$

with the class $\mathcal{K}_\infty$-function $\psi_3(\|\xi_r\|) := \frac{\varepsilon}{8}\|\xi_r\|^2$ and the following definition for the class $\mathcal{K}$-function χ:

$$\chi(\|e\|) := \sqrt{\frac{4}{\varepsilon}\left(\left[\lambda_{max}(E) + \frac{2\eta_1^2}{\varepsilon}\right]\|e\|^2\right)}$$

with $E := \frac{1}{\varepsilon}K^\top {B_r}^\top P P B_r K$ and $\eta_1 := k\left\|\check{Z}_r\right\|\|H_r\|$. Consequently, we have proven that $\dot{V}(\xi_r(t)) \leqslant -\frac{\varepsilon}{8}\|\xi_r\|^2$ when $\|\xi_r(t)\| \geqslant \chi(\|e(t)\|)$, which means that V is an ISS Lyapunov function. According to [35] the existence of a continuously differentiable ISS Lyapunov function implies ISS. Given the fact that the sector condition on $\tilde{\varphi}_r(\cdot)$ only holds locally, see Assumption 1, only local ISS can be concluded, where we can determine the bound on the initial condition $\|\xi_{r,0}\| < c_1$ using the bounds on the Lyapunov function V. According to (1), we can write

$$\|\xi_r(t)\| \leqslant \rho(\|\xi_{r,0}\|, t) + \mu\left(\sup_{\tau\in[0,t]}\|e(\tau)\|\right), \quad \forall t \geqslant 0, \tag{37}$$

with

$$\rho(\|\xi_{r,0}\|, t) = \psi_1^{-1} \circ \nu(\psi_2(\|\xi_{r,0}\|), t)$$
$$\mu\left(\sup_{\tau\in[0,t]}\|e(\tau)\|\right) = \psi_1^{-1} \circ \psi_2 \circ \chi\left(\sup_{\tau\in[0,t]}\|e(\tau)\|\right)$$

and ν a solution of the differential equation

$$\frac{d}{dt}(\nu(\|\xi_{r,0}\|, t)) = -\psi_3 \circ \psi_2^{-1}(\nu(\|\xi_{r,0}\|, t)),$$
$$\nu(\|\xi_{r,0}\|, 0) = \|\xi_{r,0}\|.$$

So as to guarantee the validity of the conditions on the nonlinearity in Assumption 1, it has to hold that $\tilde{q}_r(t) \in \mathcal{S}_a \ \forall t \geqslant 0$. Given the fact that $\tilde{q}_r = H_r\xi_r$, we have that $\|\xi_r\| < \frac{\tilde{q}_{r,a,min}}{\|H_r\|}$ with $\tilde{q}_{r,a,min} := \min(|\tilde{q}_{r,a1}|, |\tilde{q}_{r,a2}|)$, implies that $\tilde{q}_r \in \mathcal{S}_a$. So, we require that

$$\|\xi_r(t)\| \leqslant \rho(\|\xi_{r,0}\|, t) + \mu\left(\sup_{\tau\in[0,t]}\|e(\tau)\|\right) \leqslant \frac{\tilde{q}_{r,a,min}}{\|H_r\|}, \ \forall t > 0. \tag{38}$$

So as to guarantee satisfaction of (38), we require the following combined condition on the initial condition and the input $e(t)$:

$$\bar{\rho}(\|\xi_{r,0}\|) + \mu\left(\sup_{\tau\in[0,t]}\|e(\tau)\|\right) \leqslant \frac{\tilde{q}_{r,a,min}}{\|H_r\|} \tag{39}$$

with $\bar{\rho}(r) := \rho(r, 0)$ a class $\mathcal{K}$ function. By, for example, choosing in Definition 1, $c_1 = \bar{\rho}^{-1}(\alpha\frac{\tilde{q}_{r,a,min}}{\|H_r\|})$ and $c_2 = \mu^{-1}((1-\alpha)\frac{\tilde{q}_{r,a,min}}{\|H_r\|})$, with $\alpha \in (0, 1)$, it can be shown that indeed system (13) is locally input-to-state stable.

APPENDIX B: PROOF OF THEOREM 2

We will provide a concise formulation of the proof, while referring to [41] and [44] for additional details on the proof. Here, we will mainly focus on aspects related to the local nature of the result in Theorem 2. Let P_o and Q_o be positive definite matrices such that $P_o(A_{r,t} - LC_r) + (A_{r,t} - LC_r)P_o = -Q_o$ and ${G_r}^\top P_o = H_r - NC_r$ The existence of such matrices is equivalent

DOI: 10.1002/rnc

to the strict passivity of $(A_{r,t} - LC_r, G_r, H_r - NC_r, 0)$. So as to investigate the local asymptotic stability of the origin of the observer error dynamics (18), we consider the candidate Lyapunov function $V_o(e) = \frac{1}{2}e^\top P_o e$. Along solutions of (17), the derivative $\dot{V}_o$ satisfies

$$\dot{V}_o = -\frac{1}{2}e^\top Q_o e + e^\top (H_r - NC_r)^\top (\tilde{v}_r - \hat{v}_r) = -\frac{1}{2}e^\top Q_o e + (q_1 - q_2)\left(-\tilde{\varphi}_r(q_1) + \tilde{\varphi}_r(q_2)\right) \tag{40}$$

with $q_1 := H_r\xi_r$, $q_2 := (H_r - NC_r)\hat{\xi}_r + N\tilde{y}_r$, $\tilde{v}_r \in -\tilde{\varphi}_r(q_1)$ and $\hat{v}_r \in -\tilde{\varphi}_r(q_2)$. Owing to monotonicity of $\tilde{\varphi}_r(\cdot)$ for all $q_1 \in \mathcal{S}_b$ and $q_2 \in \mathcal{S}_b$, see Assumption 2, we can write $e^\top (H_r - NC_r)^\top (\tilde{v}_r - \hat{v}_r) \leqslant 0$, hence (40) yields

$$\dot{V}_o \leqslant -\frac{1}{2}e^\top Q_o e \leqslant -\frac{1}{2}\lambda_{min}(Q_o)\|e\|^2, \tag{41}$$

which implies local asymptotic (exponential) stability, given the fact that Assumption 2 only holds locally. Furthermore, it holds that

$$\|e(t)\| \leqslant \left(\frac{\lambda_{max}(P_o)}{\lambda_{min}(P_o)}\right)^{\frac{1}{2}} \|e_0\| \exp\left(-\frac{\lambda_{min}(Q_o)}{2\lambda_{max}(P_o)}t\right) \tag{42}$$

as long as $q_1(t),\ q_2(t) \in \mathcal{S}_b$. Let us investigate the bounds on $\|\xi_r(t)\|$ and $\|e(t)\|$ such that indeed $q_1(t) \in \mathcal{S}_b$ and $q_2(t) \in \mathcal{S}_b$ for all $t \geqslant 0$. First, given the fact that $q_1 = H_r\xi_r$, the requirement that $|q_1| \leqslant \tilde{q}_{r,b,min}$ is satisfied if $\|\xi_r\| \leqslant \frac{\tilde{q}_{r,b,min}}{\|H_r\|}$. Second, given the fact that $q_2 = (H_r - NC_r)\hat{\xi}_r + N\tilde{y}_r$ we rewrite the requirement $|q_2| \leqslant \tilde{q}_{r,b,min}$ as

$$\left|(H_r - NC_r)\hat{\xi}_r + N\tilde{y}_r\right| = \left|H_r(\xi_r - e) + NC_r\left(\xi_r - \hat{\xi}_r\right)\right| \leqslant \|H_r - NC_r\|\|e\| + \|H_r\|\|\xi_r\|. \tag{43}$$

Hence, we require that $\|H_r - NC_r\|\|e\| + \|H_r\|\|\xi_r\| \leqslant \tilde{q}_{r,b,min}$, which is satisfied if

$$\|\xi_r\| \leqslant \frac{\epsilon\tilde{q}_{r,b,min}}{\|H_r\|} \tag{44}$$

$$\|e\| \leqslant \frac{(1-\epsilon)\tilde{q}_{r,b,min}}{\|H_r - NC_r\|} \tag{45}$$

for some $\epsilon \in (0,1)$. Note that $H_r - NC_r \neq 0$ due to the strict passivity of $(A_{r,t} - LC_r, G_r, H_r - NC_r, 0)$. Given (42), if

$$\|e_0\| \leqslant \frac{(1-\epsilon)\tilde{q}_{r,b,min}}{\|H_r - NC_r\|}\left(\frac{\lambda_{max}(P_o)}{\lambda_{min}(P_o)}\right)^{-1/2}, \tag{46}$$

inequality (45) is valid. Note that (46) is guaranteed by the assumptions on the initial conditions in the theorem and that (44) is also implied by the conditions in the theorem.

APPENDIX C: PROOF OF THEOREM 3

According to Theorem 1, we have to satisfy (39) to obtain LISS of system (13) with respect to observer error $e(t)$. According to Theorem 2, for the system (18) to be locally exponentially stable conditions (44) and (45) have to be satisfied. The latter one is satisfied by restricting the initial conditions on the observer error as in (46). Moreover, (39) and (44) can be combined to

$$\bar{\rho}(\|\xi_{r,0}\|) + \mu\left(\sup_{\tau\in[0,t]}\|e(\tau)\|\right) \leqslant \min\left(\frac{\tilde{q}_{r,a,min}}{\|H_r\|}, \frac{\epsilon\tilde{q}_{r,b,min}}{\|H_r\|}\right).$$

DOI: 10.1002/rnc

Using (45), we can write

$$\bar{\rho}\left(\|\xi_{r,0}\|\right)+\mu\left(\frac{(1-\epsilon)\,\tilde{q}_{r,b,min}}{\|H_r-NC_r\|}\right)\leqslant\min\left(\frac{\tilde{q}_{r,a,min}}{\|H_r\|},\frac{\epsilon\tilde{q}_{r,b,min}}{\|H_r\|}\right)$$

that results in the requirement on the initial condition in ξ_r:

$$\bar{\rho}\left(\|\xi_{r,0}\|\right)\leqslant\min\left(\frac{\tilde{q}_{r,a,min}}{\|H_r\|},\frac{\epsilon\tilde{q}_{r,b,min}}{\|H_r\|}\right)-\mu\left(\frac{(1-\epsilon)\,\tilde{q}_{r,b,min}}{\|H_r-NC_r\|}\right). \tag{47}$$

The right-hand side of (47) can always be ensured to be positive, by taking ϵ sufficiently close to 1, that is, by taking $\|e_0\|$ sufficiently small. Now, inequality (47) can always be guaranteed to be valid by taking $\|\xi_{r,0}\|$ sufficiently small. So indeed for sufficiently small $\|\xi_{r,0}\|$ and $\|e_0\|$, $(\xi_r, e) = (0, 0)$ is an asymptotically stable equilibrium point of the interconnected system (13), (18); hence, this equilibrium is locally asymptotically stable.

REFERENCES

1. Deily FH, Dareing DW, Paff GH, Otrloff JE, Lynn RD. Downhole measurements of drill string forces and motions. *ASME Journal of Engineering for Industry* 1968; **90**(2):217–225.
2. Lesso B, Ignova M, Zeineddine F, Burks J, Welch B. Testing the combination of high frequency surface and downhole drilling mechanics and dynamics data under a variety of drilling conditions. *SPE/IADC Drilling Conference and Exhibition*, SPE/IADC 140347, Amsterdam, Netherlands, 2011.
3. Pavone DR, Desplans JP. Application of high sampling rate downhole measurements for analysis and cure of stick–slip in drilling. *SPE Annual Technical Conference and Exhibition*, SPE 28324, New Orleans, Louisiana, U.S.A., 1994.
4. Robnett EW, Hood JA, Heisig G, Macpherson JD. Analysis of the stick–slip phenomenon using downhole drillstring rotation data. *SPE/IADC Drilling Conference*, SPE/IADC 52821, Amsterdam, the Netherlands, 1999.
5. Jansen JD, van den Steen L. Active damping of self-excited torsional vibrations in oil-well drillstrings. *Journal of Sound and Vibration* 1995; **179**(4):647–668.
6. Serrarens AFA, van de Molengraft MJG, Kok JJ, van den Steen L. $\mathcal{H}_\infty$ control for suppressing stick–slip in oil well drillstrings. *IEEE Control Systems Magazine* 1998; **18**(2):19–30.
7. de Bruin JCA, Doris A, van de Wouw N, Heemels WPMH, Nijmeijer H. Control of mechanical motion systems with non-collocation of actuation and friction: A Popov criterion approach for input-to-state stability and set-valued nonlinearities. *Automatica* 2009; **45**(2):405–415.
8. Karkoub M, Zribi M, Elchaar L, Lamont L. Robust μ-synthesis controllers for suppressing stick–slip induced vibrations in oil well drill strings. *Multibody System Dynamics* 2010; **23**(2):191–207.
9. Halsey GW, Kyllingstad A, Kylling A. Torque feedback used to cure slip-stick motion. *Spe Annual Technical Conference and Exhibition*, SPE 18049, Houston, Texas, U.S.A., 1988.
10. Canudas-de Wit C, Rubio FR, Corchero MA. D-OSKIL: A new mechanism for controlling stick–slip oscillations in oil well drillstrings. *IEEE Transactions on Control Systems Technology* 2008; **16**(6):1177–1191.
11. Brett JF. The genesis of torsional drillstring vibrations. *SPE Drilling Engineering* 1992; **7**(3):168–174.
12. Tucker RW, Wang C. On the effective control of torsional vibrations in drilling systems. *Journal of Sound and Vibration* 1999; **224**(1):101–122.
13. Detournay E, Defourny P. A phenomenological model for the drilling action of drag bits. *International Journal of Rock Mechanics and Mining Sciences and Geomechanics Abstracts* 1992; **29**(1):13–23.
14. Richard T, Germay C, Detournay E. A simplified model to explore the root cause of stick–slip vibrations in drilling systems with drag bits. *Journal of Sound and Vibration* 2007; **305**(3):432–456.
15. Besselink B, van de Wouw N, Nijmeijer H. A semi-analytical study of stick–slip oscillations in drilling systems. *Journal of Computational and Nonlinear Dynamics* 2011; **6**(2):021006–1–021006–9.
16. Germay C, van de Wouw N, Sepulchre R, Nijmeijer H. Nonlinear drillstring dynamics analysis. *SIAM Journal on Applied Dynamical Systems* 2009; **8**(2):527–553.
17. Nandakumar K, Wiercigroch M. Stability analysis of a state dependent delayed, coupled two DOF model of drill-string vibration. *Journal of Sound and Vibration* 2013; **332**(10):2575–2592.
18. Germay C, Denoël V, Detournay E. Multiple mode analysis of the self-excited vibrations of rotary drilling systems. *Journal of Sound and Vibration* 2009; **325**(1–2):362–381.
19. Fridman E, Mondié S, Saldivar B. Bounds on the response of a drilling pipe model. *IMA Journal of Mathematical Control and Information* 2010; **27**(4):513–526.
20. Balanov AG, Janson NB, McClintock PVE, Tucker RW, Wang CHT. Bifurcation analysis of a neutral delay differential equation modelling the torsional motion of a driven drill-string. *Chaos, Solitons & Fractals* 2003; **15**(2): 381– 394.
21. Boussaada I, Mounier H, Niculescu S-I, Cela A. Analysis of drilling vibrations: a time-delay system approach. *Proceedings of the 20th Mediterranean Conference on Control and Automation*, Barcelona, Spain, 2012; 610–614.

DOI: 10.1002/rnc

22. Bresch-Pietri D, Krstic M. Adaptive output-feedback for wave PDE with anti-damping - application to surface-based control of oil drilling stick–slip instability. *Proceedings of the 53rd IEEE Conference on Decision and Control*, Los Angeles, California, U.S.A., 2014; 1295–1300.
23. Saldivar B, Mondié S, Loiseau J-J, Rasvan V. Suppressing axial-torsional coupled vibrations in drillstrings. *Journal of Control Engineering and Applied Informatics* 2013; **15**(1):3–10.
24. Kreuzer E, Steidl M. Controlling torsional vibrations of drill strings via decomposition of traveling waves. *Archive of Applied Mechanics* 2012; **82**(4):515–531.
25. Vromen TGM. Control of stick–slip vibrations in drilling systems. *Ph.D. Thesis*, 2015.
26. Perneder L, Detournay E. Steady-state solutions of a propagating borehole. *International Journal of Solids and Structures* 2013; **50**:1226 –1240.
27. Tucker RW, Wang C. Torsional vibration control and cosserat dynamics of a drill-rig assembly. *Meccanica* 2003; **38**(1):143–159.
28. Navarro-López EM. An alternative characterization of bit-sticking phenomena in a multi-degree-of-freedom controlled drillstring. *Nonlinear Analysis: Real World Applications* 2009; **10**(5):3162–3174.
29. Doris A. Controlling vibrations in a drilling system. *Patent* 2012; **WO/2012/084886 Al**.
30. Doris A. Method and system for controlling vibrations in a drilling system. *Patent* 2013; **WO/2013/076184 A2**.
31. Dwars S. Recent advances in soft torque rotary systems. *SPE/IADC Drilling Conference and Exhibition*, SPE/IADC 173037, London, United Kingdom, 2015.
32. Runia DJ, Grauwmans R, Stulemeijer I. A brief history on the Shell 'soft torque rotary system' and some recent case studies. In *Second International Colloquium on Nonlinear Dynamics and Control of Deep Drilling Systems*, van de Wouw N, Detournay E (eds).: Eindhoven, The Netherlands, 2012; 69–76.
33. Nessjøen PJ, Kyllingstad A, D'Ambrosio P, Fonseca IS, Garcia A, Levy B. Field experience with an active stick–slip prevention system. *SPE/IADC Drilling Conference and Exhibition*, SPE/IADC 139956, Amsterdam, Netherlands, 2011.
34. Vromen TGM, van de Wouw N, Doris A, Astrid P, Nijmeijer H. Observer-based output-feedback control to eliminate torsional drill-string vibrations. *Proceedings of the 53rd IEEE Conference on Decision and Control*, Los Angeles, California, U.S.A., 2014; 872–877.
35. Sontag ED, Wang Y. On characterizations of the input-to-state stability property. *Systems and Control Letters* 1995; **24**(5):351–259.
36. Sontag ED, Wang Y. New characterizations of input-to-state stability. *IEEE Transactions on Automatic Control* 1996; **41**(9):1283–1294.
37. Wen JT. Time domain and frequency domain conditions for strict positive realness. *IEEE Transactions on Automatic Control* 1988; **33**(10):988–992.
38. Kyllingstad A, Nessjøen PJ. A new stick–slip prevention system. *SPE/IADC Drilling Conference and Exhibition*, SPE/IADC 199660, Amsterdam, Netherlands, 2009.
39. Grauwmans R, Stulemeijer I. Drilling efficiency optimization: vibration study. *Presentation Shell Exploration and Production*, Rijswijk, the Netherlands, 2009.
40. Besselink B, van de Wouw N, Nijmeijer H. Model reduction for nonlinear systems with incremental gain or passivity properties. *Automatica* 2013; **49**(4):861–872.
41. Doris A, Juloski AL, Mihajlović N, Heemels WPMH, van de Wouw N, Nijmeijer H. Observer designs for experimental non-smooth and discontinuous systems. *IEEE Transactions on Control Systems Technology* 2008; **16**(6): 1323–1332.
42. Sturm JF. Using SeDuMi 1.02, A MATLAB toolbox for optimization over symmetric cones. *Optimization Methods and Software* 1999; **11**(1–4):625–653.
43. Löfberg J. YALMIP : a toolbox for modeling and optimization in MATLAB. *Proceedings of the IEEE International Symposion on Computer Aided Control Systems Design*, Taipei, Taiwan, 2004; 284–289.
44. Heemels WPMH, Juloski AL, Brogliato B. Observer design for Lur'e systems with monotone multi-valued mappings. *Proceedings of the 16th IFAC World Congress on Automatic Control*, Prague, Czech Republic, 2005.

DOI: 10.1002/rnc